

Engineering autoantibody capturing polymer beads and its application for blood filtration in autoimmune disease

A thesis submitted by

Doyeon Koo

in partial fulfillment of the requirements for the degree of

Master of Science

in

Bioengineering

Tufts University

[May, 2017]

Adviser: Dr. Qiaobing Xu

ProQuest Number:10277109

All rights reserved

INFORMATION TO ALL USERS

The quality of this reproduction is dependent upon the quality of the copy submitted.

In the unlikely event that the author did not send a complete manuscript and there are missing pages, these will be noted. Also, if material had to be removed, a note will indicate the deletion.



ProQuest 10277109

Published by ProQuest LLC (2017). Copyright of the Dissertation is held by the Author.

All rights reserved.

This work is protected against unauthorized copying under Title 17, United States Code
Microform Edition © ProQuest LLC.

ProQuest LLC.
789 East Eisenhower Parkway
P.O. Box 1346
Ann Arbor, MI 48106 – 1346

Abstract

In autoimmune disease patients, immune system intensifies the production of autoantibodies, including Antinuclear antibodies (ANAs). Some patients with elevated level of ANAs take immunosuppressive drugs and receive hemodialysis to remove excess fluid, waste substances and ANAs. However, the current problem in hemodialysis is that it excessively removes necessary proteins and antibodies. This study describes a new technique to engineer polymer beads to capture ANAs in the patient blood. The beads are conjugated with HEp-2 cell nuclear proteins in which ANAs have binding specificity to. This new technique allows autoantibodies to be 'fished-out' during the dialysis process, providing an effective therapy for patients. The result showed that the microbeads can significantly capture ANAs in ANA positive human serum. The microbeads captured 29.2 μg of ANAs per cm^2 surface area of the beads. Application of the beads in dialysis makes dialysis process to be a cost and time efficient therapy.

Acknowledgements

I would like first to express my gratitude to my supervisor Dr. Qiaobing Xu, my research advisor. He always provided me useful comments and remarks. His enthusiasm to guide us always inspired me. His office door was always opened, and he always answered my questions during this thesis experiment. Without his support, I could not finish my master's thesis.

I would also like to thank my thesis committee faculties: Dr. James Van Deventer (Department of Chemical Engineering, Tufts University) and Dr. Xiaocheng Jiang (Department of Biomedical Engineering, Tufts University).

I want to acknowledge all the lab members at Xu lab: Yamin, Tao, Yuki, Zach, Caleb, Prudence, Tom, Justin, and Liu. Without your help, I was not able to finish up my project. Thank you for always answering my questions and finding reagents or chemicals for me. I especially thank Yuki and Tao, who have worked with me for the past semesters.

Finally, I express my very profound gratitude to my parents, Jakyu Koo and Okkyung Park, and my older brother, Bonho Koo, for the support they provided me in the past 27 years. Your sacrifice and love are the most valuable lesson I have learned throughout my entire life. I also thank my roommate, Jacklyn, and my boyfriend, Inseung, for always being there for me. This accomplishment would not be possible without them. Thank you everyone. I truly enjoyed my life in Boston and my life as a master's student. Peace out!

Doyeon Koo

Table of contents:

Chapter 1: INTRODUCTION

1.1. Autoimmune Disease	
1.1.1. Background	pg. 2
1.1.2. Pathogenesis of Autoimmune Disease	pg. 2
1.2. Antinuclear antibody and HEp-2 cells	
1.2.1. Antinuclear antibody in autoimmune disease	pg. 3
1.2.2. HEp-2 cells and antinuclear antibody	pg. 4
1.3. Current Diagnosis for autoimmune disease	
1.3.1. Mechanism of current diagnostic methods	pg. 5
1.4. Current treatments for autoimmune disease	
1.4.1. Replacement or immunosuppressive therapy	pg. 7
1.4.2. Limitation of current treatments	pg. 8
1.5. Application of blood filtration for treating disease	pg. 9
1.6. Diffusion in dialysis	pg. 10
1.7. Antigen and antibody binding kinetics	pg. 12
1.8. Study Object	
1.8.1. The motivation	pg. 13
1.8.2. The concept	pg. 14
1.8.3. The project scheme	pg. 15

Chapter 2: METHODS

2.1. Introduction	pg. 17
2.2. Activation of polystyrene carboxyl microbeads	pg. 17
2.3. HEp-2 cell culture	pg. 18
2.4. HEp-2 cell nuclear protein extraction	pg. 18
2.5. ELISA assay of nuclear protein	pg. 19
2.6. Nuclear protein conjugation to the microbeads	pg. 21

2.7. Capturing of antinuclear antibody using nuclear protein conjugated microbeads	pg. 22
2.8. Qualitative analysis of microbead's efficiency in capturing antinuclear antibody	pg. 24
2.9. Quantitation of fluorescence intensity	
2.9.1. Fluorescence intensity measurement	pg. 25
2.9.2. Percent of beads with fluorescence signal	pg. 25
2.10. Statistical analysis	
2.10.1. ELISA assay analysis	pg. 26
2.10.2. Microbead system analysis	pg. 26

Chapter 3: RESULTS

3.1. Activation of the microbeads	pg. 27
3.2. Extracted nuclear protein concentration	pg. 29
3.3. Nuclear protein specificity to antinuclear antibody – ELISA	pg. 30
3.4. validation of nuclear protein conjugation to the microbeads	pg. 34
3.5. Capturing antinuclear antibody using microbeads	pg. 37
3.6. Fluorescence image analysis	
3.6.1. Fluorescence intensity of each image	pg. 39
3.6.2. Percent of beads showing fluorescence	pg. 42
3.7. Efficiency of microbeads in capturing ANAs	
3.7.1. Calculation of microbead surface area	pg. 44
3.7.2. Change in ANA concentration difference before and after incubation with the microbeads	pg. 44
3.7.3. Concentration of ANA per cm ² of microbeads surface	pg. 45
3.7.4. Comparison of ANA capturing efficiency between ELISA and microbeads	pg. 46

Chapter 4: DISCUSSIONS

- 4.1. Extracted nuclear protein from HEp-2 cells pg. 48
- 4.2. Determination of specificity between nuclear protein and ANA pg. 49
- 4.3. Nuclear protein conjugation to the microbeads pg. 50
- 4.4. Detection of ANA using the microbeads pg. 50
- 4.5. Qualitative analysis of the microbead's binding capacity pg. 51

Chapter 5: CONCLUSION pg. 54

Chapter 6: FUTURE WORK

- 6.1. Application of microbeads in a blood filtration device pg. 55
- 6.2. Analysis of ANA types captured by microbeads pg. 55
- 6.3. Application with different nuclear proteins pg. 56
- 6.4. Change of coupling buffer and incubation apparatus pg. 56

Reference pg. 57

List of Figures:

Figure 1: Image of test glass slide in IFA technique	pg. 6
Figure 2: Image of stained nucleus in IFA technique	pg. 6
Figure 3: The mechanism of standard hemodialysis	pg. 9
Figure 4: The diffusion mechanism of hemodialysis	pg. 11
Figure 5: The overall scheme of this project in long term	pg. 14
Figure 6: The overall concept of this project	pg. 15
Figure 7: The experimental procedure of this study	pg. 15
Figure 8: Procedure of Indirect ELISA assay	pg. 21
Figure 9: Procedure of developing microbeads to capture ANAs	pg. 23
Figure 10: General mechanism of EDC/NHS reaction	pg. 27
Figure 11: Mechanism of coupling cell lysate to amine functioned beads	pg. 28
Figure 12: Mechanism of coupling protein to amine functionalized beads	pg. 28
Figure 13: GFP protein coupled to the microbeads after activation by EDC/NHS reaction	pg. 29
Figure 14: Standard curve for BCA assay	pg. 30
Figure 15: Standard curve for ELISA assay	pg. 31
Figure 16: ELISA assay showing specificity of nuclear protein to ANA	pg. 32
Figure 17: ELISA assay showing the specificity of nuclear protein to ANA and to anti-B-actin antibody	pg. 33
Figure 18: Fluorescence and overlay images of microbeads with no nuclear protein	pg. 35

Figure 19: Fluorescence and overlay images of the anti-B-actin–nuclear protein–microbeads complex	pg. 36
Figure 20: Effect of decreasing nuclear protein concentration on the microbead’s capturing capacity of ANA	pg. 38
Figure 21: Comparison between microbeads conjugated with equal amount of nuclear protein in capturing ANA positive and negative antibodies	pg. 39
Figure 22: Fluorescence intensity and standard deviation of images	pg. 41

List of Tables:

Table 1: The price of currently marketed drugs for autoimmune disease	pg. 8
Table 2: Percentage of microbeads with fluorescence signal	pg. 43
Table 3: Number of beads and surface area corresponding to the mass of microbeads	pg. 44
Table 4: Change in concentration of ANA before and after incubation with the microbeads	pg. 44
Table 5: Concentration of ANA per cm^2 of microbeads surface area	pg. 45
Table 6: Concentration of captured ANA positive per cm^2 of microbeads surface area	pg. 46
Table 7: Concentration of captured ANA negative per cm^2 of microbeads surface area	pg. 46
Table 8: Comparison between the microbeads and ELISA assay in capturing ANAs	pg. 47

Engineering autoantibody capturing polymer beads and its application for blood filtration in autoimmune disease

CHAPTER 1

INTRODUCTION

1.1. Autoimmune Disease

1.1.1. Background

According to National Institute of Health (NIH), 23.5 million people are currently suffering from the autoimmune disease in the United States (Autoimmune statistics, AARDA). The epidemiological study states that autoimmune diseases are the 10th cause of death in developing countries (Chandrashekara, 2012). There are more than 80 types of autoimmune diseases, and the most common diseases are Rheumatoid Arthritis (RA), Systemic Lupus Erythematosus (SLE), Multiple sclerosis (MS). In 2005, approximately 1.5 million of the US adults were diagnosed with RA and most of them were in the age range of 40-60 years (Teo et al., 2012). In 2008, around 0.3 million of the US adults had definite SLE and more than 90% of cases of SLE were occurred in women (MS statistics). It affects in all ages, from infancy to old age.

The immune response involved is not a one step process but instead is very complicated. Thus, the condition of autoimmune disease patients can fluctuate easily, and the cause of disease varies by patients.

1.1.2. Pathogenesis of Autoimmune Disease

Autoimmune disease is defined as a condition in which the immune system attacks own cells in the body and cause tissue destruction or organ malfunction

because autoantigens are treated as a foreign substance (Moscarello et al., 2007). In autoimmune disease patients, the citrullinated proteins are recognized as a foreign substance by the immune system. Activated protein-arginine deiminase enzymes trigger the production of autoantigens that signal an immune response of an organism against its own cells and tissues (Darrah et al., 2012). The autoantigens interact with lymphocytes and activate self-reactive lymphocytes that cause the destruction of tissue and cells. The autoantigens can initiate, terminate and intensify the autoimmunity by depositing immune complexes in tissue, leading to a further destruction of an organ (Lange S et al., 2011). Thus, autoimmune disease patients usually have a high level of autoantibodies due to intensified immune system. For example, RA, SLE, and MS are caused due to over-activation of the immune system that produces autoantibodies beyond the normal level. In these patients, autoantibodies attach to and damage nerve, joint and tissue cells (Kuwana et al., 2002).

There has been a significant progress in understanding autoimmunity and the fundamental cause of abnormal immune response. However, the mechanism that causes autoimmune diseases is still not completely understood.

1.2. Antinuclear Antibody and HEp-2 Cells

1.2.1. Antinuclear Antibody in Autoimmune Diseases

Antinuclear antibodies (ANA) are a group of autoantibodies characterized by specificity for numerous antigenic determinants of cell nuclei. In autoimmune

disease patients, ANA to human proteins, also known as autoantigens, are produced and ANAs bind to the contents of cell nucleus. The most common ANAs are anti-Ro, anti-centromere, anti-histone and anti-dsDNA antibodies (Kavanaugh et al., 2000).

As immune system intensifies the production of autoantibodies, high level of ANA attach to tissue and nerve cells to destruct them. The pathogenic role of ANA in autoimmune disease is still under investigation but they have been used as disease markers, primarily for diagnostic screening and to monitor the course of associated tissue disease (Tan et al., 1989). The currently available ANA diagnostic methodologies are Enzyme Linked Immunosorbent Assay (ELISA), Dot Blot and the Indirect Fluorescent Antibody (IFA) technique.

1.2.2. HEp-2 Cells and Antinuclear Antibody

HEp-2 cells, a human epithelial type 2 cells, are widely used for ANA detection because ANA has high specificity to nuclear fraction of HEp-2 cells. The large size of HEp-2 cells and high rate of mitosis allow a broad range of antibody detection, including anti-centromere and anti-Ro antibodies (Keren, 2002). HEp-2 substrates are usually fixed on a glass slide or microtiter plate, and ANA binds to the nucleus of the cells. This results in various patterns of HEp-2 cell nuclear staining. Specific types of autoantibodies are associated with each pattern. For example, homogeneous pattern is associated with anti-histone antibodies, speckled pattern is associated with anti-Ro and centromere pattern is associated with anti-centromere antibodies (Sack et al., 2009).

1.3. Current Diagnosis for Autoimmune Disease

1.3.1. Mechanism of Current Diagnostic Methods

The most widely used diagnostic methodologies for autoimmune disease are autoantibody test, ANA test, blood cell count, and C-reactive protein test. Among these tests, indirect fluorescent antibody (IFA) technique using HEp-2 cells remains the gold standard of diagnosis (Sato et al., 2009). ELISA and Dot Blot tests can detect a single specific autoantigen from a cell lysate, however, have lower sensitivity than IFA (Sato). IFA allows the nuclear staining pattern with high sensitivity, and can screen multiple types of autoantibody simultaneously.

To detect ANA using IFA, a patient blood is collected and serum is separated after clotting to avoid hemolysis. On the slide or plate coated with HEp-2 cell substrate, patient serum is loaded for 30 minutes at room temperature. After thorough wash, fluorescent anti-human antibody conjugate is applied. ANAs bound to HEp-2 cell substrate will be conjugated with this secondary antibody. By imaging the slide under a fluorescence microscope, nuclear staining pattern can be observed as shown in Figure 1 and 2 (MBL International).

In addition to ANA IFA technique, recent studies have developed multiplex immunoassays (Sato et al., 2000). The principle of multiplex ANA assay is similar to IFA but instead of glass slides, magnetic beads are used. The patient serum is incubated in a well containing mixture of bead suspension and the fluorescence level is measured by an automated immunoassay analyzer. These beads generally use recombinant or purified antigens to detect specific autoantibodies. Multiplex

assay has an advantage of cost and labor effectiveness and quick availability of test results (Xu et al., 2007).

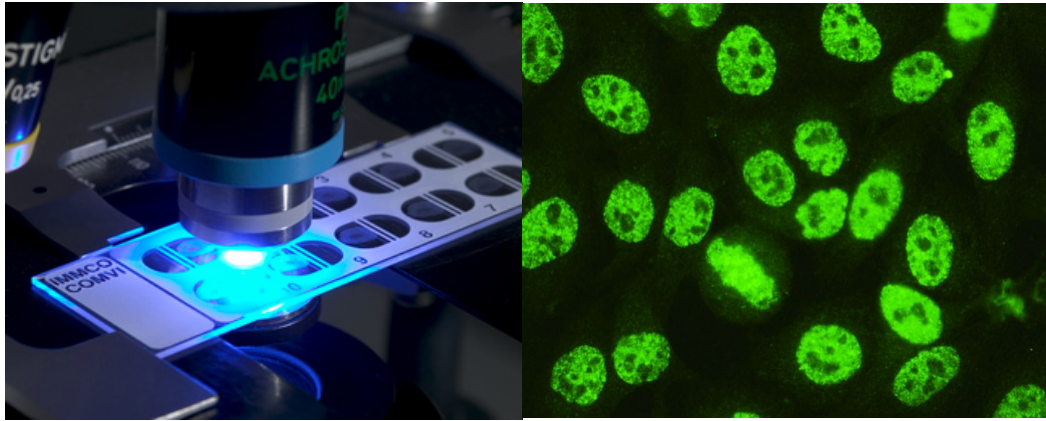


Figure 1 and 2 Image of Test Glass Slide (left) and Nucleus Staining by ANA in IFA Technique. The glass slide on the left has HEp-2 cell substrate coated. Once patient serum containing ANA is loaded, the nucleus of HEp-2 substrate is stained as shown in image on the right.

Although IFA and multiplex immunoassay can show specific autoantibodies present in the patient serum by nuclear staining, there are a few limitations in these tests. First, the interpretation of IFA test result is subjective because the fluorescent intensity is determined by the human eyes (Satoh). In the presence of strong fluorescence stain, the weak fluorescence signal can be easily ignored. Also, the signal is dependent on the concentration of fluorescent conjugate and on the ANA concentration. In this case, specific ANAs with low concentrations cannot be detected through IFA. Second, the staining pattern in IFA may not always accurately reflect the location of target antigen. Some antigens are present in the multiple location inside a cell. For example, anti-Ro antibodies can bind to both nuclei and cytoplasm (Satoh). Thus, it is difficult to determine whether specific ANAs are bound correctly to the targeted antigen site.

1.4. Current Treatments for Autoimmune Disease

1.4.1. Replacement or Immunosuppressive Therapy

Currently there are two approaches to treat autoimmune diseases. The first is a conservative approach: hormone replacement, blood transfusions or symptomatic therapy. The second is an immunosuppressive or immunomodulation therapy, which are more aggressive and painful for patients (Buchner et al., 2014). An example of replacement therapy is thyroxine medication for patients with autoimmune thyroid disease (Premawardhana, 2006). These patients take regular doses of thyroxine because their immune system reduces the production of thyroid hormone. As an example of immunosuppressive therapy, patients with SLE take immunosuppressive medications, such as azathioprine (Imuran) and mycophenolate (Cellcept) to downregulate the immune response by disrupting DNA synthesis to prohibit cell divisions (Lauren Martz, 2015). However, because these drugs suppress the entire immune system, patients are at an increased risk for infection and cancer development (Schmidt et al., 2007). This treatment can be effective for short-term, but the condition of patients can easily relapse without chronic treatment. Also, severe side effects include diabetes mellitus, osteoporosis, bone marrow suppression, and pancreatitis (Heneghan et al., 2002).

1.4.2. Limitation of Current Treatments

Recent study revealed that 10% to 15% of autoimmune disease patients appear to be unresponsive to immunosuppressive therapy (Heneghan). Alternative treatment for these patients is a dialysis in conjunction with immunosuppressant

medication to remove waste substance and excess fluid and to regulate immune response concurrently (Hayashi et al., 2001). For example, patients with SLE and RA undergo the impairment of renal function due to ANAs destructing tissue cells in kidney. For these patients, routine dialysis is required to adjust the volume of fluid and to remove excess waste substances (Kronbichler et al., 2013). However, during the dialysis process, the ANAs along with necessary antibodies and other important proteins are removed from the blood. Despite a prolonged remission of the disease, the patients are at a lack of antibodies required to protect from infections and must take supplementary medications to fulfill the lost proteins.

Furthermore, the current price of marketed drugs is very expensive as shown in Table 1.

Table 1 The Price of Currently Marketed Drugs for Autoimmune Disease

Enbrel (Amgen, Pfizer)	RA	>> \$ 1000 / syringe
Humira (Abbvie, Eisaid Co.)	RA	
Benlysta belimumab (GSK)	SLE	\$ 500 / vial
Avonex (Biogen)	MS	\$ 5895 /kit

For example, Humira (40mg/0.8ml), a common drug for RA and SLE patients, is more than \$2000 for 2 syringes. Enbrel to treat RA also costs around \$1500 for 2 syringes (www.pharmacychecker.com). Benlysta belimumab for SLE costs \$2995 for 6 vials. (<http://www.goodrx.com/benlysta>). Avonex for MS costs \$5895 for intramuscular kit (<http://www.drugs.com/price-guide/avonex-pen>). Therefore, there is a need to develop cheaper and safer alternatives that can both diagnose and regulate the level of autoantibodies instantaneously.

1.5. Application of Blood Filtration for Disease Treatment

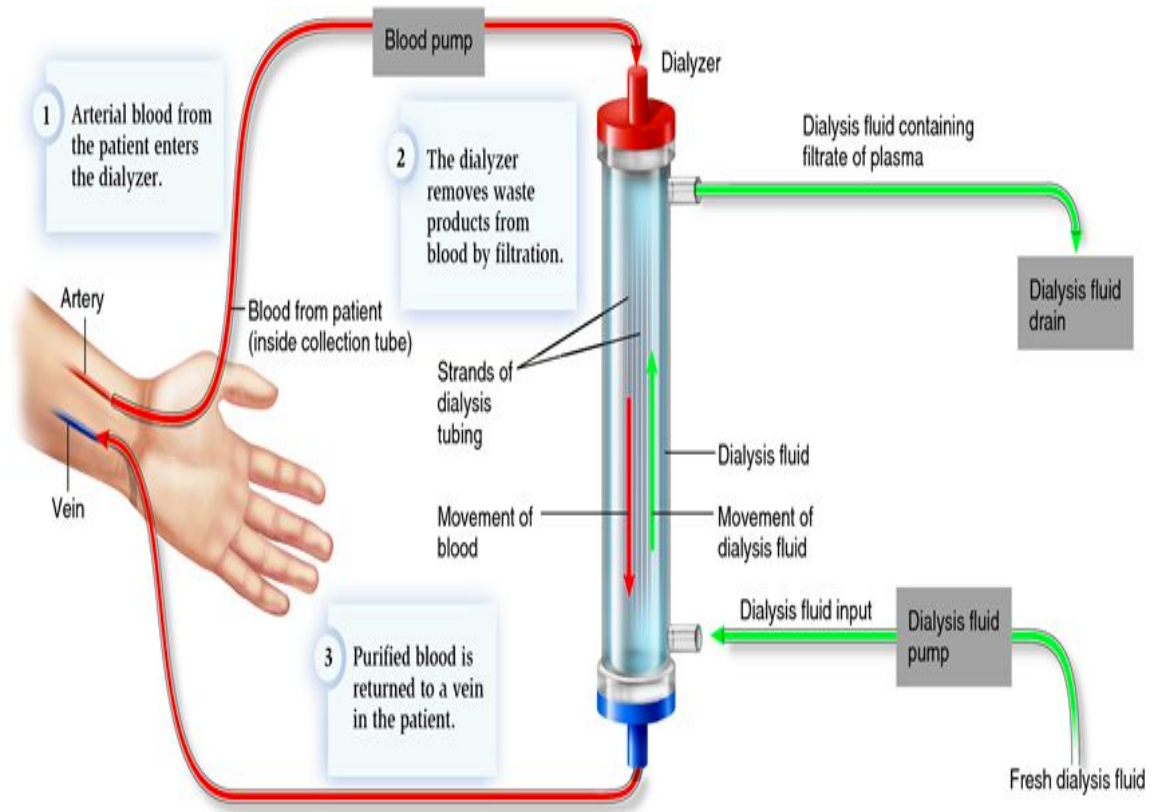


Figure 3 The mechanism of standard hemodialysis. The blood first enters the dialyzer. The membrane inside the dialyzer filters waste products and excessive fluids. Purified blood is then returned to a vein in the patient. Each dialysis takes about 3 ~ 4 hours and patients receive it three times a week.

Autoimmune disease patients usually have increased immune complex deposition in the kidney that damages tissue cells. In conjunction with drug treatment, patients suffering from the impairment of kidney receive dialysis three times a week (Marrack et al., 2001). The mechanism of hemodialysis is that patient serum enters the dialyzer, the membrane inside the device filters out waste products, and the purified blood is returned to a vein in the patient as shown in Figure 3

(drSatishd.com). SLE patients, among other autoimmune disease patients, are the most susceptible to kidney failure. These patients are recommended to receive dialysis to control hypertension, reduce inflammation and remove autoantibodies (Hauser et al., 2008).

However, the major problem with the use of hemodialysis, especially in autoimmune disease patient, is that it removes necessary antibodies and proteins in the blood (Cucchiari et al., 2013). Autoimmune disease patients have low immunity during immunosuppressive therapy that inhibits the production of autoantibodies. As the dialysis additionally removes plasma factors that are essential in activating immune system, patients are at risk of getting infected. Also, patients after standard dialysis suffer from hypertension or hypotension, bone diseases, depression and lost appetite (Dasgupta, 2000).

Thus, there is a need to develop a new system that can only filter out autoantibodies instead of the entire plasma factors in the blood during dialysis. By filtering out autoantibodies, the accumulation of immune complex can be prevented and the kidney function can be restored much faster. Also, the patients do not have to take chronic immunosuppressive medication along with dialysis to balance out the immune complexes.

1.6. Diffusion in Dialysis

In dialysis, the main force of determining the rate of filtering the blood out is the concentration gradient. Outside of the dialyzer filter has no proteins. The

blood entering dialyzer has high concentration of antibodies and proteins. Due to the concentration gradient inside and outside of the dialyzer, the substances inside the dialyzer diffuses out to the outer membrane as shown in Figure 4 (GAMBRO, 2007). When the concentration inside and outside of the dialyzer filter reaches equilibrium, the purified blood enters back to the vein of a patient.

Hemodialysis: Diffusion

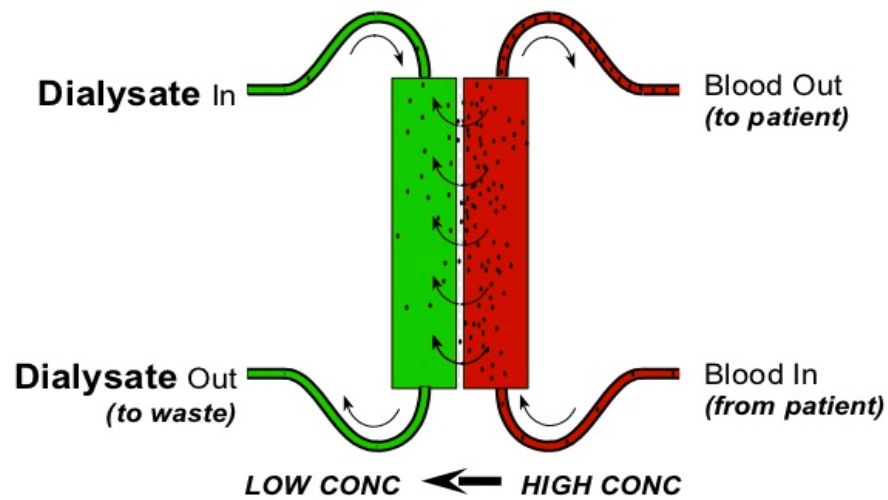


Figure 4 The diffusion mechanism of hemodialysis

The rate of how rapidly these substances are moving across the membrane is a flux, expressed in the amount of substance per unit area per unit time. The flux equation is shown below (Ronco et al., 1998).

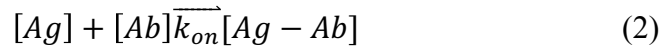
$$Jd = D \times A \times T \times \frac{dc}{dx} \quad (1)$$

where, dx is membrane thickness, T is temperature, A is surface area of membrane and D is diffusivity coefficient of solute.

Here, the diffusivity coefficient of the solute represents how fast a substance can diffuse across a solvent volume. This depends on the viscosity of solvent, radius of particles and the number of particles per mole.

1.7. Antigen and Antibody Binding Kinetics

The antigens and antibody bind together depending on their physical state, affinity and specificity to each other. In the solution containing free antigen and free antibodies, they bind to each other at specific rate called the association rate constant. The dissociation rate constant is the affinity of reverse reaction where antigens and antibodies dissociate from each other. The specificity between antigen and antibody is called the association binding constant. For HEp-2 cell antigens and ANAs, the affinity of interaction can be written as the following Equation 2 (Goldberg, 1952).



where, [Ag] is antigen concentration, [Ab] is ANA concentration and [Ag-Ab] is antigen-antibody complex concentration.

The association binding constant K_a can be written as the following Equation 3 (Goldberg).

$$K_a = \frac{[Ag-Ab]}{[Ag][Ab]} \quad (3)$$

In the interaction between HEp-2 cell and ANAs, the major factors affecting its affinity is the concentration of ANAs present in the patient serum and the concentration of HEp-2 cell substrates. Due to presence of other antibodies in the

normal human serum, the concentration of ANAs must be high enough to form antigen-antibody complex with HEp-2 cell antigens.

1.8. Study Objectives

1.8.1. The Motivation

This study primarily focuses on designing and developing microbeads which captures and ‘fishes out’ antinuclear antibodies in autoimmune disease patient serum. This allows the clinicians to regulate immune response by decreasing the elevated level of autoantibodies in the blood.

The motivation that drove the development of this microbead system was to provide a new and potentially more effective approach to treat autoimmune diseases. By using microbeads, the burden of drug costs can be reduced, the diagnosis procedure can be simple and the patients may avoid side effects of immunosuppressive drugs. As patients with autoimmune disease receive dialysis on regular basis, the application of microbeads in dialysis system can allow them to control autoimmunity, as well as monitor the progress of disease.

In addition, the microbeads are conjugated with native antigens from nuclear fractions of HEp-2 cells, instead of recombinant antibody. As HEp-2 cell substrates are known to contain more than 50 types of autoantigens, the microbeads can detect several ANAs concurrently (Copple et al., 2007). This reduces the production cost and due to the use of native antigens, the reactivity with ANA will provide a better understanding of autoimmunity. The microbeads can be used

multiple times and can be coupled with other types of antigens that are specific to each patient to monitor the progression of the autoimmune diseases.

1.8.2. The Concept

Polystyrene carboxyl microbeads are conjugated with HEp-2 cell nuclear proteins and these beads are incubated with ANA positive human serum to capture ANAs. This system is alike IFA in detecting the ANAs but instead the microbeads can capture antibodies and filter them out to reduce the elevated level of ANAs in autoimmune disease patients. The developed microbeads will be applied to the dialysis device. Figure 5 and 6 shows the overall scheme of this study.

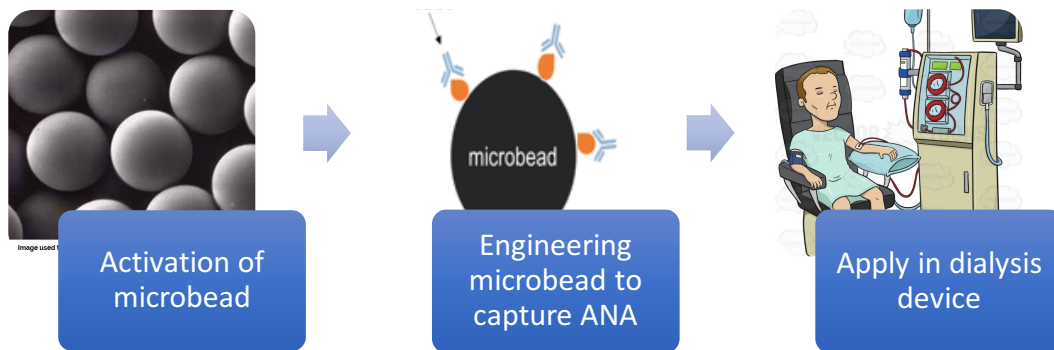


Figure 5 The overall scheme of this project. First, the beads will be engineered to capture antinuclear antibodies. After confirming the specificity and stability of the beads are confirmed, the beads are applied inside the dialysis device.

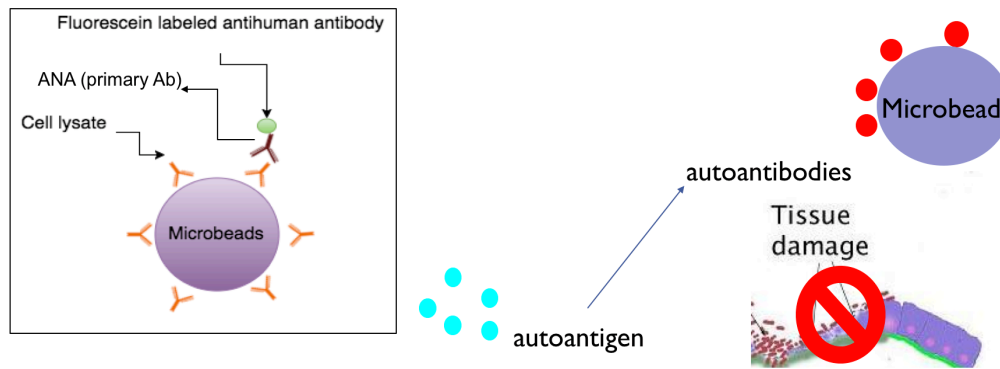


Figure 6 The Overall Scheme of this Study. Microbeads that are coupled with nuclear protein from HEp-2 cell lysate are used to capture antinuclear antibodies in the patient serum. The anti-human secondary antibody-FITC labeled can be used to detect the antibodies bound on the surface of microbeads.

1.8.3. The Project Scheme

This study was divided into three major experiments: activation of microbead, ELISA assay to validate specificity of nuclear protein to ANA, and application of microbead to capture ANA as shown in Figure 7.

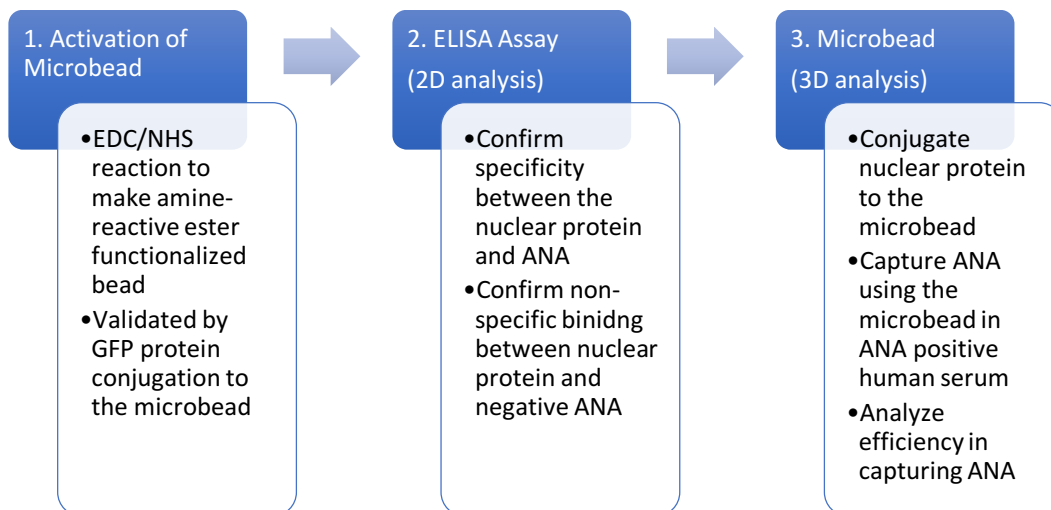


Figure 7 The experimental procedure of this study. Each step is necessary to perform the following step.

The hypothesis of the first part is that microbeads are activated by EDC/NHS reaction and positive charged proteins can bind to its surface. If GFP proteins cannot bind to the surface, the microbeads cannot be coupled with nuclear proteins.

The hypothesis of the second part is that nuclear protein has a significantly higher binding specificity to ANA than other proteins. The non-specific binding between nuclear protein and negative ANAs should not be observed to proceed to the third part.

The hypothesis of the last part is that microbeads coupled with nuclear protein can effectively capture ANA in ANA positive human serum than in ANA negative human serum.

CHAPTER 2

METHODS

2.1. Introduction

The study was broken into three major experiments to develop microbeads that can capture antinuclear antibody (ANA) in autoimmune disease patient serum. First, the microbeads had to be activated to conjugate the protein to the surface and the blocking efficiency had to be validated to prevent non-specific binding to the microbeads. Secondly, the nuclear protein had to be extracted from HEp-2 cells and its specificity to ANA had to be measured in two-dimensional assay, such as ELISA. Lastly, the nuclear protein was conjugated to the microbeads to measure the specificity and capacity of microbeads in capturing ANA.

2.2. Activation of Polystyrene Carboxyl Microbead

To activate the surface of microbeads, 30 mg of 250 μm microbeads were incubated in EDC/NHS reaction buffer: 85 mM 1-Ethyl-3-(3-dimethylaminopropyl) carbodiimide (EDC; Sigma-Aldrich, St. Louis, MO) and 85 mM N-Hydroxysuccinimide (NHS; Sigma) in phosphate buffered saline (PBS; Fisher Scientific, Pittsburgh, PA). Following 4 hours of incubation, the beads were washed with DI water three times to remove excess EDC and NHS. To confirm the activation of microbead, the beads were incubated with GFP protein. Following

overnight incubation at 4 °C, the beads were thoroughly washed with PBS and imaged by a fluorescent microscope (Keyence, Itasca, IL).

2.3. HEp-2 Cell Culture

HEp-2 cells (ATCC, Manassas, VA) were cultured in Dulbecco's modified Eagle's medium (DMEM; Gibco, Grand Island, NY) supplemented with 10% fetal bovine serum (FBS; Gibco), and 100 units/mL penicillin streptomycin (Pen Strep; Gibco). In a T175 Corning flask (Sigma), 5×10^6 cells were seeded. The media was changed every three days and the cells were harvested at 100% confluency. To harvest cells, cells were first washed with 5ml of PBS. A 3 ml of trypsin was added to the flask and incubated for 5 minutes. To stop the reaction, 6 ml of culture medium was added. The solution containing HEp-2 cells were transferred to a 15-ml falcon tube and centrifuged down at 1000 rpm for 10 minutes to remove debris.

2.4. HEp-2 Cell Nuclear Protein Extraction

For nuclei isolation, cells were harvested from flask, washed with PBS and resuspended in ice-cold hypotonic buffer N (10 mM Hepes pH 7.5, 2mM MgCl₂, 25 mM KCl) containing 1 mM PMSF and 1mM DTT. Supernatant was discarded and the cells were resuspended in 10 volume of ice-cold hypotonic buffer N containing 1mM DTT and protease inhibitors. After 30 minutes of incubation on ice, the cells

were homogenized by vortexing and continuously monitored under phase contrast microscope until 95% of cells were lysed. To the cell lysate, 125 μ l of 2M sucrose solution per ml of lysate was added and centrifuged at 1000 rpm for 10 minutes. Supernatant was discarded and the pellet was resuspended in 5 ml of ice-cold buffer N (10 mM Hepes pH 7.5, 2mM $MgCl_2$, 25 mM KCl, 250 mM sucrose) containing 1mM DTT, 1mM PMSF, and protease inhibitors. The solution was centrifuged at 1000 rpm for 10 minutes, 4 °C. The supernatant was discarded and nuclei was resuspended in PBS.

The amount of nuclear protein collected was measured by determining protein concentration using Thermo Scientific Pierce BCA Protein Assay (Fisher Scientific). Bovine Serum Albumin (2mg/ml, Fisher Scientific) was used as standard.

2.5. ELISA Assay of Nuclear Protein

To confirm the presence of nuclear protein and its specificity to antinuclear antibodies, an indirect Enzyme Linked Immunosorbent assay (ELISA) was developed. The nuclear protein was diluted to various concentrations in 100 mM bicarbonate/carbonate coating buffer: 160, 80, 40, 20 μ g/ml. The wells of a Nunc Maxisorp Flat-Bottom 96 well plate (Fisher Scientific) were coated with nuclear protein by pipetting 50 μ l of the diluted protein into the plate in three replicates. The plate was covered with adhesive plastic and was incubated at 4 °C overnight. The plate was washed three times by filling the wells with 200 μ l PBS. The solution

was completely removed by flicking the plate over a sink. The remaining protein-binding site was blocked by adding 200 μl of 5% bovine serum albumin (BSA; Sigma-Aldrich) in PBS to each well. After overnight incubation at 4 °C, the plate was washed with PBS three times. To each well, 100 μl of antinuclear antibody positive human serum (ANA positive; MBL International, Woburn, MA) was added and incubated overnight at 4 °C. For negative control, 100 μl of antinuclear antibody negative serum (ANA negative; MBL International) was added. For positive control, 100 μl of monoclonal anti- β -actin produced in mouse (anti- β -actin; Sigma Aldrich) at the concentration of 0.8 $\mu\text{g/ml}$ was added to the well. Following three times of wash with PBS, 100 μl of 0.5 $\mu\text{g/ml}$ anti-human-IgG-HRP conjugated secondary antibody (MBL International) was added to the wells containing the nuclear proteins and negative controls. For positive control wells, 100 μl of 0.5 $\mu\text{g/ml}$ anti-mouse-IgG-HRP conjugated secondary antibody was added. Following 2 hours of incubation at room temperature, the plate was washed three times with PBS and 100 μl of 1-StepTM Ultra TMB Substrate Solution (TMB; Thermo Fisher) was added to each well. After 30 minutes of incubation at room temperature, 100 μl stop solution for TMB substrates (STOP; Thermo Fisher) was added and the absorbance was quantified at 450 nm by a plate reader (Molecular Devices, CA).

Figure 8 shows a procedure of the second part of this study.

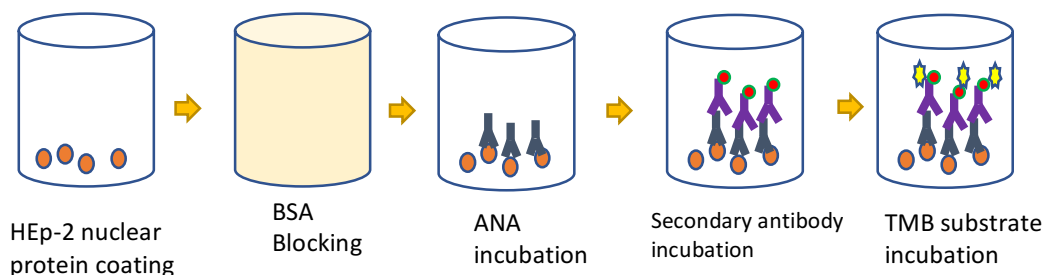


Figure 8 Procedure of Indirect ELISA Assay. HEp-2 nuclear proteins are coated into each well. The remaining binding sites are blocked by 5% BSA. ANA is incubated to be bound to nuclear proteins. The amount of ANA is detected by anti-human-IgG-HRP conjugate.

To generate a standard curve, known concentrations of anti- β -actin (Sigma Aldrich) were coated into each well of the same plate: 0, 2, 4, 8, 16, 40, 60 $\mu\text{g/ml}$. These wells were also washed with PBS, blocked with 5% BSA and incubated with 100 μl of anti-mouse-IgG-HRP conjugated secondary antibody overnight at 4 $^{\circ}\text{C}$. After wash, 100 μl of TMB substrates were added to each well and 100 μl of stop solution was added after 30 minutes of incubation at room temperature. The absorbance was quantified at 450 nm by a plate reader.

2.6. Nuclear Protein Conjugation to the Microbead

To conjugate nuclear protein to the microbead, the microbead was first activated as described in 2.2. After thorough wash with water, the microbeads were incubated overnight in a 1.7 mL microcentrifuge tube (Fisher Scientific) at 4 $^{\circ}\text{C}$ with 600 $\mu\text{g/ml}$ nuclear protein diluted in PBS. As a negative control, 0 $\mu\text{g/ml}$ nuclear protein was incubated with microbead and as a positive control 80 $\mu\text{g/ml}$ anti- β -actin antibodies were incubated with the beads. All groups of microbeads

were then washed with PBS three times and incubated with 1 ml of 5% BSA solution to block remaining binding sites. The blocking buffer was removed after overnight incubation at 4 °C, followed by three times of PBS wash.

To validate that proteins are conjugated to the microbead, the beads conjugated with nuclear protein and the negative control beads were incubated with 400 μ l of 0.8 μ g/ml anti- β -actin antibodies overnight at 4 °C, while the positive control beads were incubated with 400 μ l of anti-mouse-IgG-FITC labeled antibodies (Sigma) overnight at 4 °C. The beads were washed again with PBS three times. The positive control was imaged by a fluorescent microscope. The negative control and nuclear protein conjugated beads were incubated with 400 μ l of anti-mouse-IgG-FITC labeled antibodies overnight at 4 °C. Following three times of PBS wash, both sample groups were imaged by a fluorescent microscope to confirm proteins are conjugated to the microbeads.

2.7. Capturing of Antinuclear Antibody Using Nuclear Protein Conjugated Microbeads

To capture ANA using nuclear protein conjugated microbeads, 40 mg of microbeads were activated as described in 2.2. The beads were washed by water three times, and each of 10 mg microbeads incubated with different concentrations of nuclear protein: 3000, 600, 300 μ g/ml. After overnight incubation at 4 °C, the beads were washed with PBS three times again. To block the remaining protein binding sites, the beads were incubated with 5% BSA in PBS overnight at 4 °C.

Followed by wash with PBS, the beads were then incubated with ANA positive human serum (MBL International). For negative control, 10 mg of beads were conjugated with 3 mg/ml of nuclear protein and incubated with ANA negative human serum (MBL International) overnight at 4 °C. The beads were washed with PBS and incubated with anti-human-IgG-FITC (MBL International) overnight at 4 °C. Following three times of wash with PBS, the beads were imaged by a fluorescent microscope to quantify microbead's capturing capability. This experimental step was repeated three times and one image was selected per each condition.

The experimental scheme is illustrated in Figure 9 as shown below.

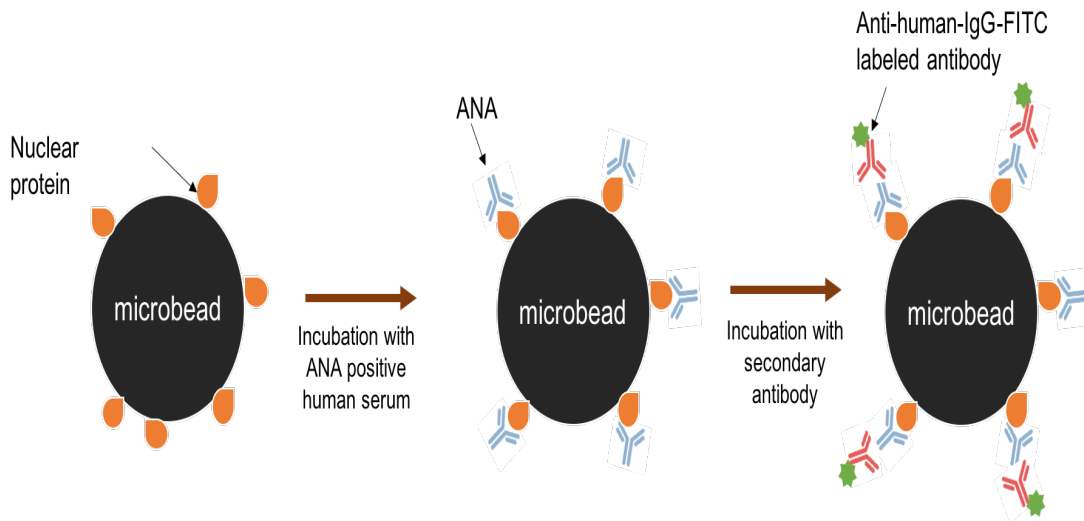


Figure 9 Procedure for developing microbeads to capture ANA in human serum. Microbeads are coupled with HEP-2 nuclear proteins. ANA binds to antigens in nuclear proteins and detected by anti-human-IgG-FITC labeled antibody.

2.8. Qualitative Analysis of Microbead's Efficiency in Capturing Antinuclear Antibody

Two sets of 4.5mg, 9 mg, 15 mg microbeads were activated individually as described in 2.2. All beads were then incubated with 1 ml of 2 mg/ml nuclear proteins overnight at 4 °C. The protein solution was removed and the beads were washed with PBS three times. Each set of beads were then incubated with 300 µl of 4 mg/ml ANA positive human serum and 300 µl of 4 mg/ml ANA negative human serum (negative control). After overnight incubation at 4 °C, the serum was removed from the well and its concentration was measured by Thermo Scientific Pierce BCA Protein Assay. The protein concentration change before and after incubation of ANA human serum was calculated.

To analyze the efficiency of beads in capturing ANAs, the surface area of the microbeads had to be calculated using the following equation according to the manufacturer's protocol.

$$\text{Surface area of particles: } A = \frac{6W}{PD} \times 10^4 \quad (4)$$

where, W is weight of microbead in gram, P is density of bead polymer (polystyrene = 1.05), and D is diameter of a bead in µm (250 µm).

The number of beads in each group was also calculated based on the manufacturer's protocol.

$$\text{Number of particles: } N = \frac{6W}{3.14 * P * D^3} \times 10^{12} \quad (5)$$

where, W is weight of microbead in gram, P is density of bead polymer (polystyrene = 1.05), and D is diameter of a bead in μm (250 μm).

The difference in protein concentration before and after incubation was divided by the surface area of each group. This gives the concentration of ANA that can be captured per each cm^2 .

To compare this result, the binding capacity of ELISA assay was also calculated. The concentration of captured ANA in each condition was divided by the working area of each well (2.7 cm^2). This gives the concentration of ANA that can be captured per each cm^2 .

2.9. Quantitation of Fluorescence Intensity

2.9.1 Fluorescence Intensity Measurement

Fluorescence intensity in each image was analyzed by ImageJ (National Institute of Health, Maryland). Using the program built-in function, the background was removed by adjusting the color threshold of each image. The mean fluorescence intensity and standard deviation of each image was then measured.

2.9.2 Percent of Beads Captured ANA

The percentage of beads that showed fluorescence in each group was analyzed for coupling efficiency. The total number of beads in each group was

counted from the fluorescence image. Using the ImageJ program, the beads that show fluorescence above threshold was then counted. To calculate the percentage, the number of beads that showed fluorescence was divided by the total number of beads in each group.

2.10. Statistical analysis

2.10.1. ELISA Assay Analysis

Statistical differences in ELISA assay was calculated by Analysis of Variance (ANOVA): Two Factor with Replication at the confidence level of 0.95 and defined the statistical significance as a p-value less than 0.05. The concentration of ANA in the well incubated with 0 $\mu\text{g/ml}$ was defined as 0 $\mu\text{g/ml}$. The error bars represent a 5% of means from each group.

2.10.2. Microbead System Analysis

Statistical differences in the number of microbeads and the concentration of ANA captured (positive vs. negative) was calculated by a two-way ANOVA with confidence level of 0.95 and defined statistical significance as p-value less than 0.05. The error bars represent a 5% of means from each group.

CHAPTER 3:

RESULTS

3.1. Activation of the Microbeads

The microbeads were activated by 1-ethyl-3-(3-dimethylaminopropyl) carbodiimide hydrochloride (EDC) / N-hydroxysuccinimide (NHS) reaction. In EDC/NHS reaction, carboxyl group on the microbeads form an intermediate called o-Acylisourea with EDC. With the addition of NHS, the intermediate becomes a stable amine-reactive ester as shown in Figure 10. The primary amine on nuclear protein from cell lysate then forms a stable amide bond with the amine-reactive ester, being conjugated to the bead's surface as shown in Figure 11 (Thermo Fisher).

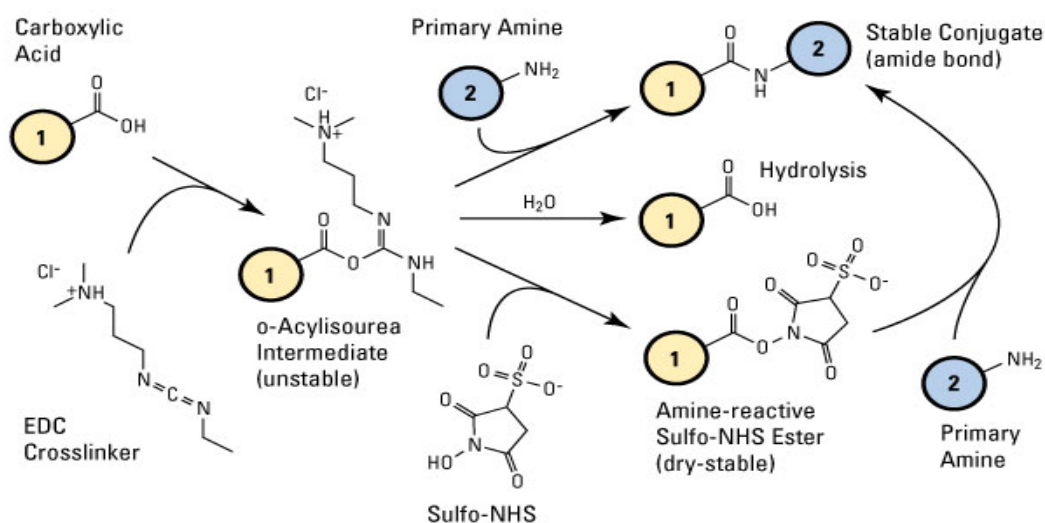


Figure 10 General Mechanism of EDC/NHS reaction. EDC reacts with carboxylic acid and forms o-Acylisourea which is an unstable intermediate. With the addition of NHS, this complex becomes a stable amine-reactive ester. The primary amine of nuclear protein then reacts with the amine-reactive ester complex.

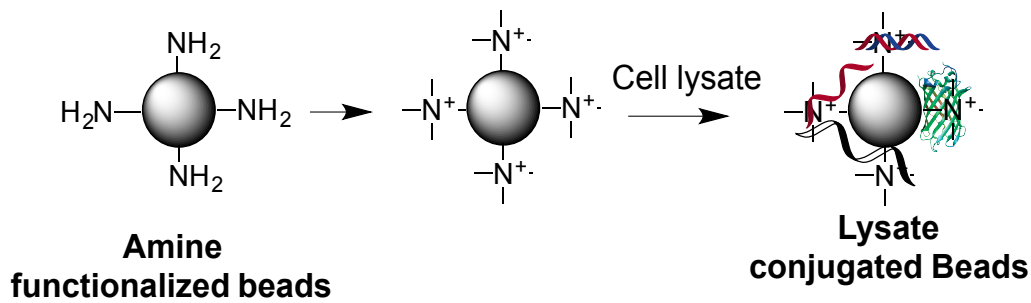


Figure 11 Mechanism of coupling cell lysate to amine functionalized beads. Through EDC/NHS reaction, the surface of amine functionalized beads become positively charged. The cell lysate which is negatively charged can bind to the surface of beads.

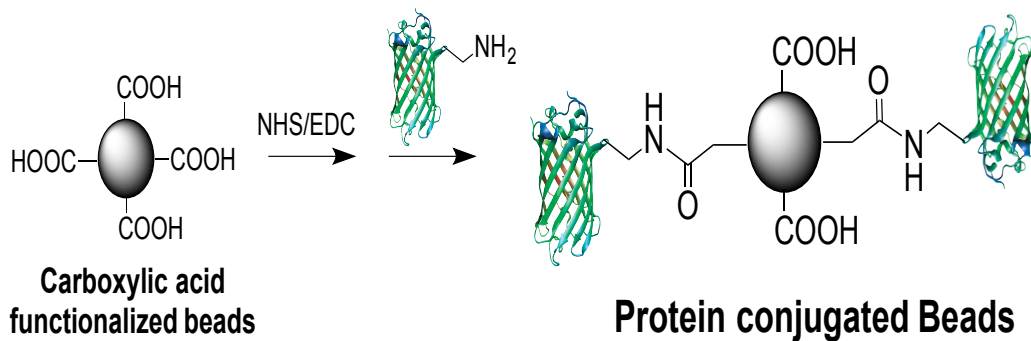


Figure 12 Mechanism of coupling protein to amine functionalized beads. EDC/NHS reaction forms an amine-reactive ester on the surface of carboxylic functionalized beads. The protein then reacts with primary amine to be coupled to the beads.

To validate the activation of microbeads, GFP proteins were conjugated to the bead upon EDC/NHS reaction as shown in Figure 12. If the carboxyl group of the bead has successfully formed a stable intermediate by EDC/NHS, the protein can form a stable amide bond and be conjugated to the surface of bead.

As shown in Figure 13, the beads that show green fluorescence around its surface represent that GFP proteins are successfully conjugated to the bead. Some beads do not show fluorescence because the conjugation efficiency was not high

enough. This fluorescence indicates that the protein has been conjugated to the bead's surface by the amide bond.

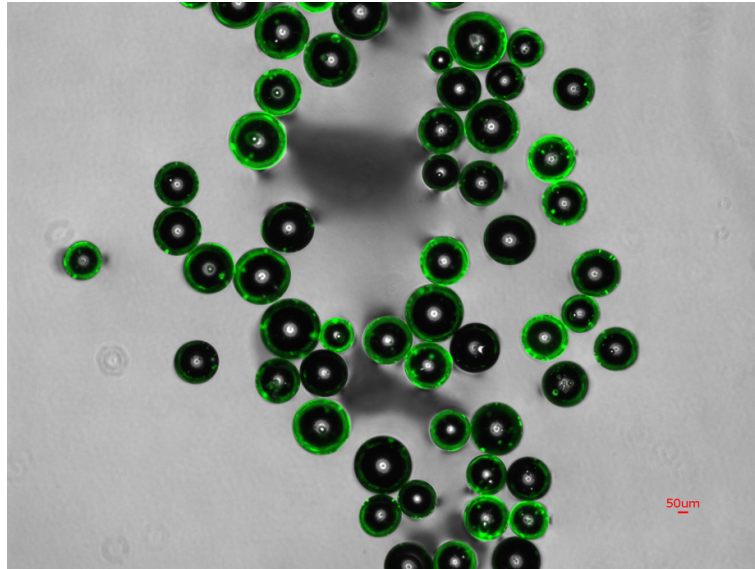


Figure 13 GFP protein coupled to the microbeads after activation by EDC/NHS reaction.

3.2. Extracted Nuclear Protein Concentration

The concentration of extracted nuclear protein was measured by comparing the assay response of a sample to that of a standard whose concentration is known using a standard curve in Figure 14. The standard curve equation was obtained by linear regression. The absorbance of protein was interpolated on the regression line to calculate its concentration. The concentration of nuclear protein was determined to be 3 mg/ml. This represents that the cell lysis procedure was successful to yield a high concentration of nuclear protein.

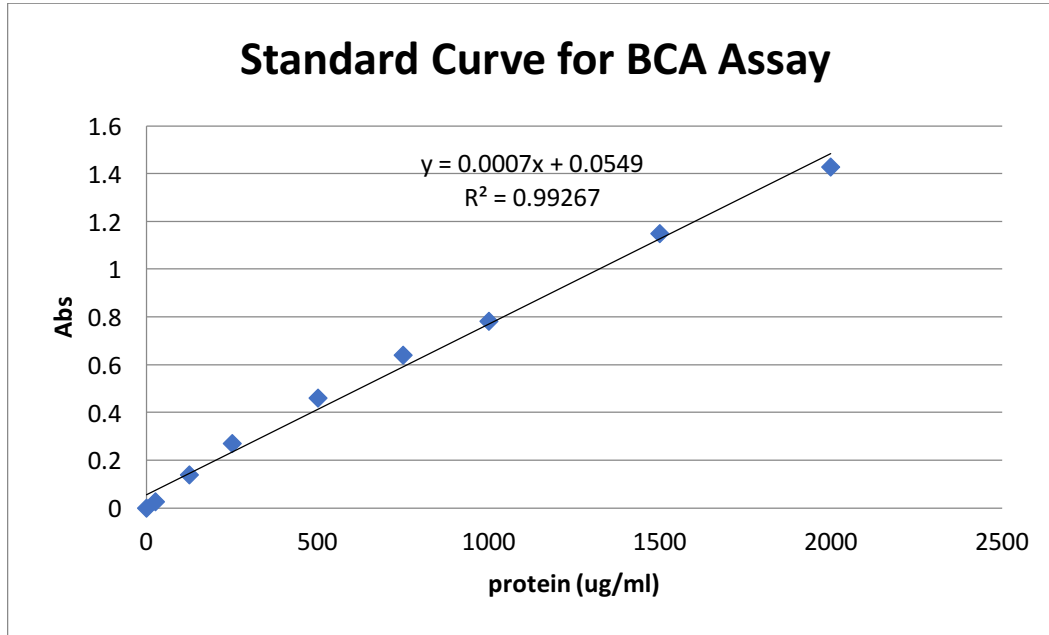


Figure 14 Standard Curve for BCA Assay to Determine the Concentration of nuclear proteins extracted from HEp-2 cell lysate. The Standard curve was obtained by using known concentrations of Bovine Serum Albumin solution. The R^2 value of 0.99 represents that the data points are correlated to each other.

3.3. Nuclear Protein Specificity to Antinuclear Antibody – ELISA

The second part of this study was Indirect Enzyme-Linked Immunosorbent Assay (ELISA) to analyze the specificity of HEp-2 cell nuclear proteins to human serum containing ANAs. Extracted nuclear proteins were coated onto microplate, then primary antibody, ANA positive human serum, was added to each well. ANAs were bound to coated proteins and detected by anti-human-IgG-FITC labeled secondary antibodies. This process was to validate the idea of this study in two-dimensions, whether obtained ANA positive human serum has specificity to the HEp-2 cell nuclear proteins in our lab.

First, the concentration of antibody concentration in each well was measured by comparing the assay response of a sample to that of a standard whose concentration is known using a standard curve in Figure 15. The standard curve was presented in logarithmic scale and the equation was plotted by linear regression.

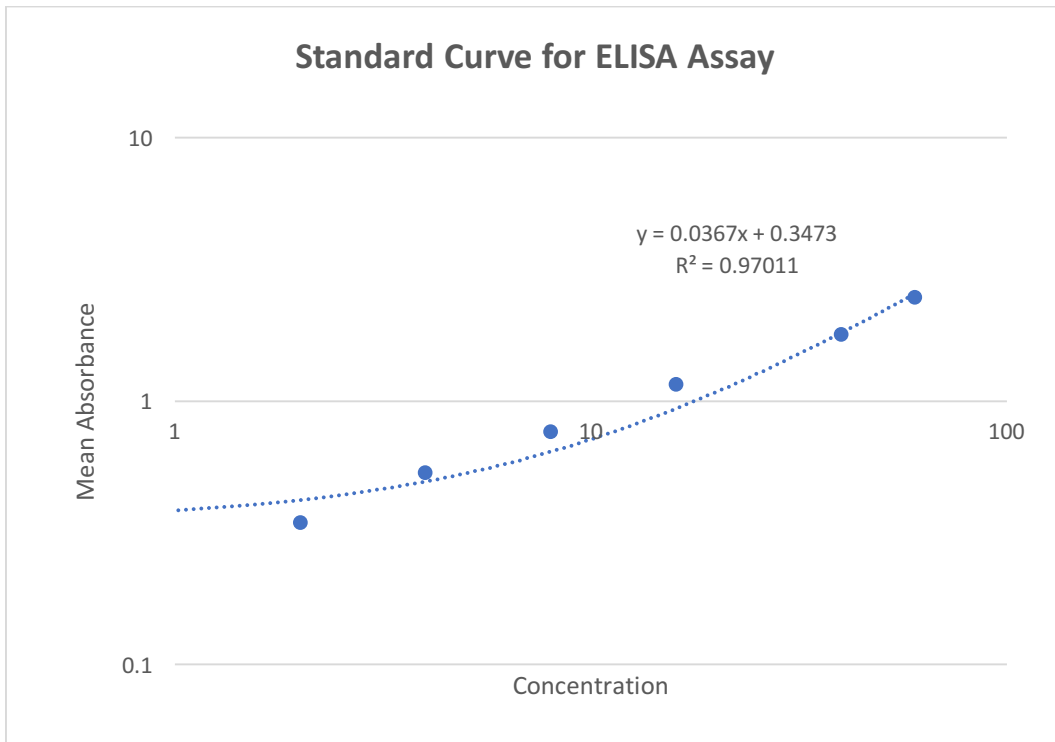


Figure 15 Standard Curve for ELISA Assay to Determine the Concentration of Captured ANA. The Standard curve was obtained by using known concentrations of anti-beta-actin antibodies. The graph represented in logarithmic scale and the R^2 value of 0.97 represents that the data points are correlated to each other.

The absorbance of antibody was interpolated on the regression line to calculate its concentration. The concentration of ANA positive captured by nuclear protein was determined to be 22.40, 27.29, 38.59, 53.19 $\mu\text{g/ml}$ for microbeads incubated with 20, 40, 80, 160 $\mu\text{g/ml}$ nuclear proteins respectively as shown in

Figure 16. The concentration of ANA negative captured by nuclear protein was determined to be 4.96, 5.86, 7.80, 8.08 $\mu\text{g/ml}$ for microbeads incubated with 20, 40, 80, 160 $\mu\text{g/ml}$ nuclear proteins respectively.

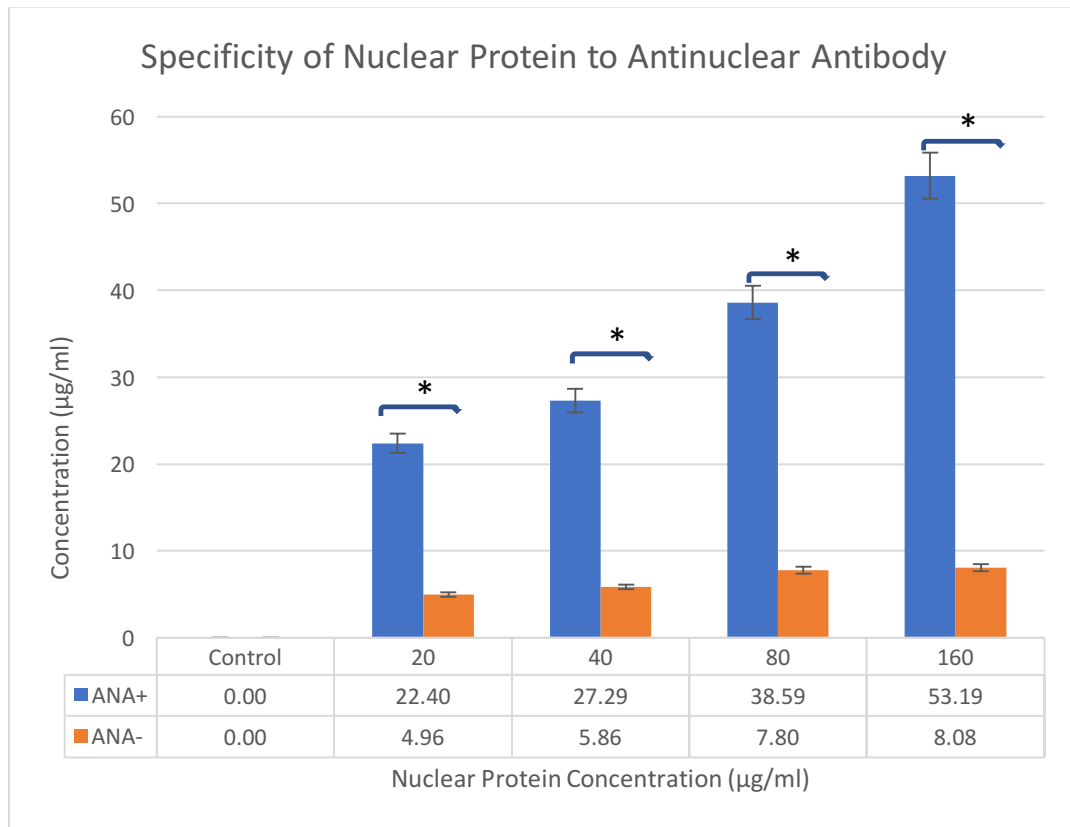


Figure 16 ELISA Assay Result that shows the specificity of Nuclear Protein to Antinuclear Antibody. The error bars represent 5% of mean from three samples per treatment regimen. The concentration of ANA captured by 0 $\mu\text{g/ml}$ nuclear proteins was determined to be 0. The asterisk represents significant difference between the control and the concentration of ANA in nuclear protein coated wells.

It was observed that as the concentration of nuclear protein increases, the amount of ANA that can be captured also increases. Nuclear protein of 160 $\mu\text{g/ml}$ could detect 53.19 $\mu\text{g/ml}$ of positive ANA. The specificity of nuclear protein to negative ANAs was also observed but the number of antibodies captured in each well did not increase despite the nuclear protein concentration increased. The

highest concentration of negative control was 8.08 $\mu\text{g/ml}$ detected by 160 $\mu\text{g/ml}$ of nuclear protein. This was lower than the positive ANA detected by lowest concentration of nuclear protein, 20 $\mu\text{g/ml}$. The p-value for effect of ANA positive and negative incubation with nuclear protein was 0.037.

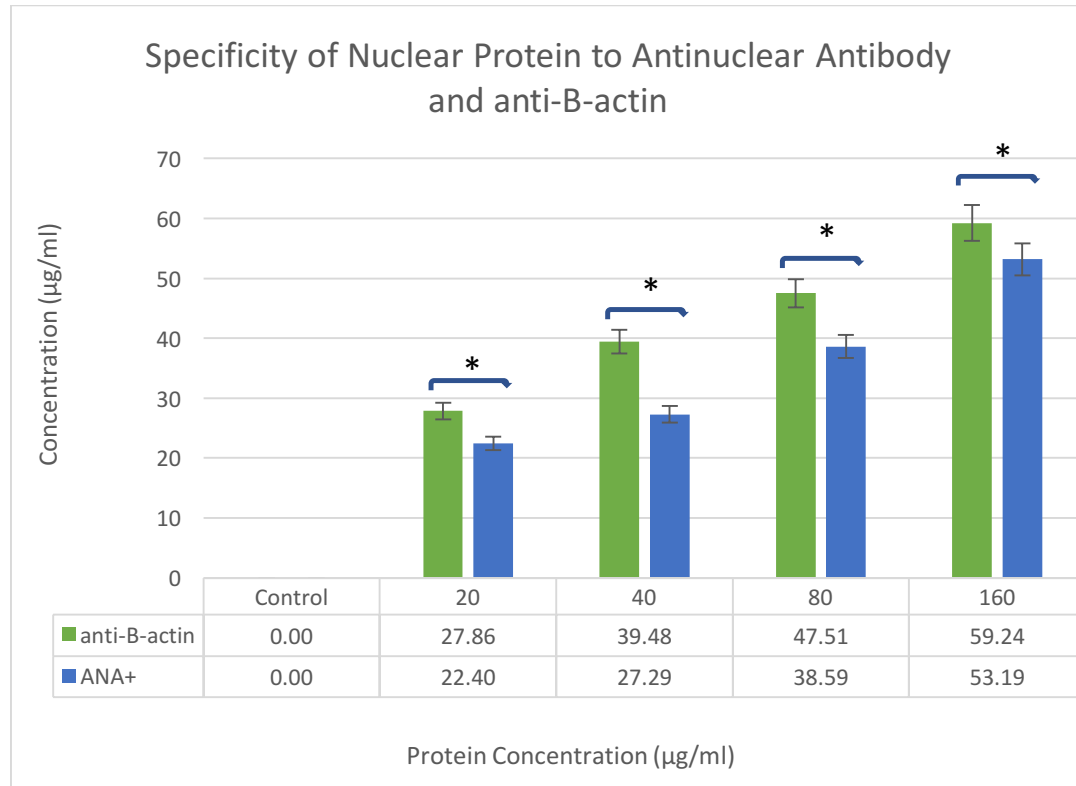


Figure 17 ELISA Assay Result that shows the specificity of Nuclear Protein to Antinuclear Antibody and to anti-B-actin antibody respectively. The error bars represent 5% of mean from three samples per treatment regimen. The concentration of antibodies captured by 0 $\mu\text{g/ml}$ nuclear proteins was determined to be 0. The asterisk represents significant difference between the control and the concentration of antibodies in nuclear protein coated wells.

As a positive control, the specificity of nuclear protein to positive ANA was compared to that of anti- β -actin antibodies. The concentration of anti- β -actin captured by nuclear proteins were determined to be 27.86, 39.48, 47.51 and 59.24 $\mu\text{g/ml}$ for each treatment as shown in Figure 17. The concentration of anti- β -actin

antibodies also increased as the concentration of nuclear proteins increased. In all treatments, the concentration of anti- β -actin antibody was higher than positive ANA and the highest concentration was 59.24 $\mu\text{g/ml}$ captured by 160 $\mu\text{g/ml}$ of nuclear proteins. The difference between the positive control, anti-beta-actin, and ANA positive was small in this graph because the concentration of anti-beta-actin coated in each well was lower than the nuclear proteins. If the concentration was the same for both anti-beta-actin and the nuclear protein, the positive control may have higher specificity. This shows that the presence of nuclear protein in the extracted cell lysate and that anti-beta-actin can be used as positive control in examining microbeads coupling efficiency.

3.4. Validation of Nuclear Protein Conjugation to the Microbeads

The third part was to analyze the efficiency of microbeads conjugated with HEp-2 nuclear protein to capture ANAs. This was a three-dimensional study of the second part. The process was the same, except the nuclear proteins were coated on the surface of microbeads.

Microbeads were divided into two groups to validate blocking and conjugation efficiency. First, the beads were incubated without nuclear protein, blocked with 5% BSA and incubated with primary antibody, anti- β -actin, followed by secondary antibody-FITC labeled to detect fluorescence signal from microbead complexes.

As shown in Figure 18, the beads incubated without the bead had no fluorescence. The images were taken under white and fluorescence filters separately to clearly visualize the location of beads. This indicates that the blocking was efficient to prevent non-specific binding of the bead. After activation of the bead, if the beads are not conjugated with protein and blocked with BSA, no other proteins can bind to the surface of beads.

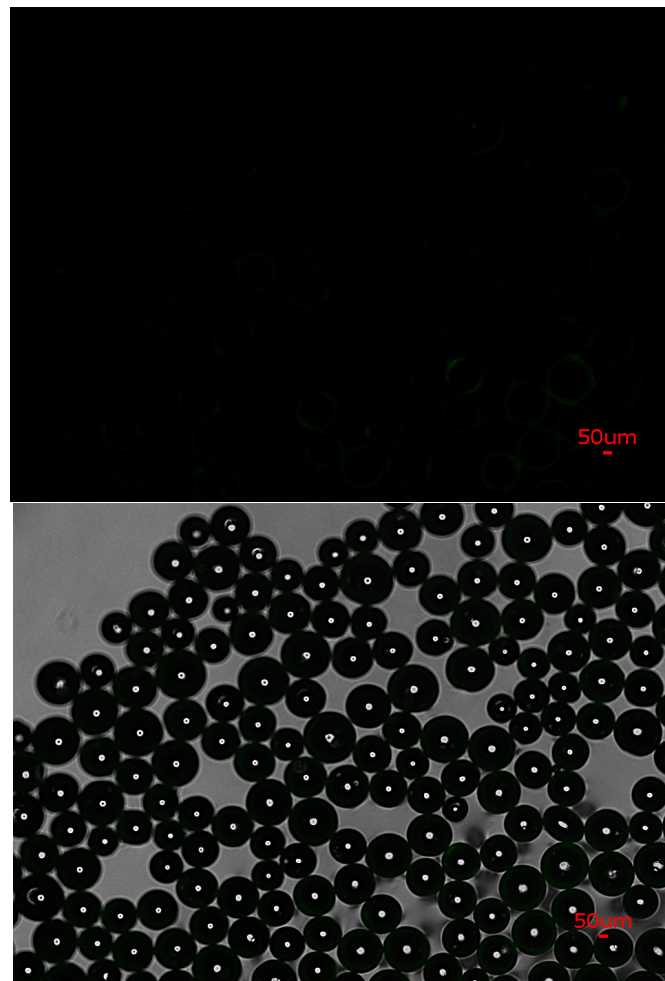


Figure 18 Fluorescence and Overlay Images of microbead with no nuclear protein to confirm blocking efficiency. The microbeads show no fluorescence because no proteins were bound to the surface of microbeads after blocking with 5% BSA solution.

To quantify the conjugation efficiency, the beads were incubated with 0.6 mg/ml nuclear protein. After blocking with 5% BSA, the beads were incubated with anti- β -actin primary antibodies, followed by FITC-labeled secondary antibody. As shown in Figure 19, the fluorescence signal was observed from the beads, indicating that the intermediate formed by EDC/NHS coupled with primary amines in HEP-2 cell nuclear proteins.

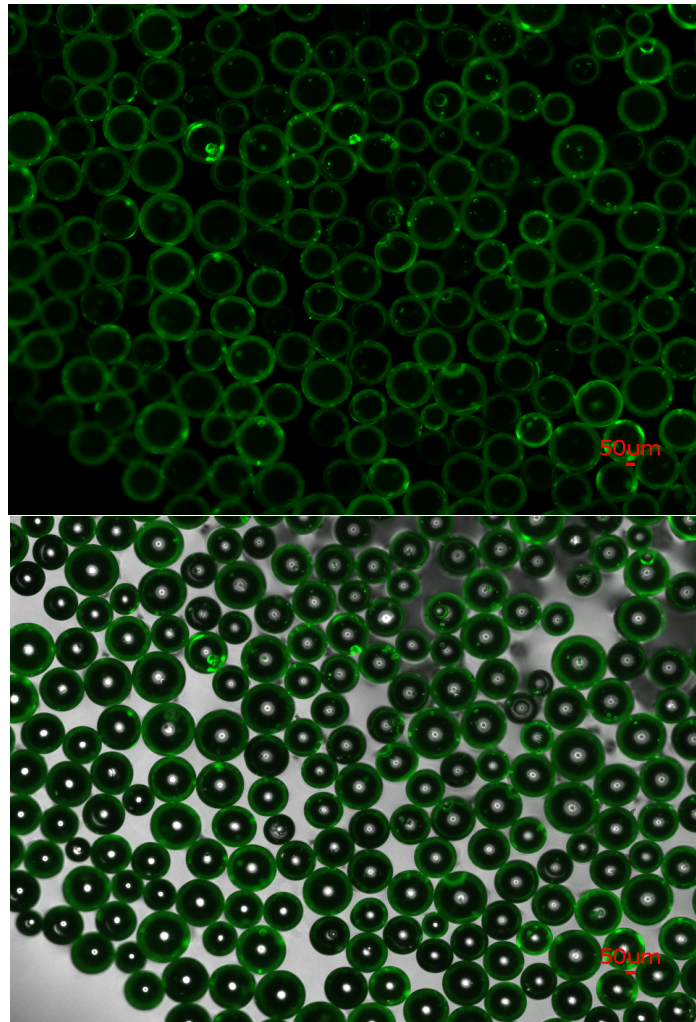


Figure 19 Fluorescence and overlay image of the anti-B-actin – nuclear protein – microbead complex detected by FITC-labeled secondary antibody. The beads that show fluorescence signal captured anti-B-actin antibodies.

3.5. Capturing Antinuclear Antibody using Microbeads

The microbeads conjugated with nuclear proteins were utilized to capture ANA in autoimmune disease patient serum. To observe the effect of nuclear protein concentration on capturing specificity, the beads were conjugated with different concentrations of nuclear protein: 3 mg/ml, 0.6 mg/ml, 0.3 mg/ml. As shown in Figure 20, all groups showed fluorescence, indicating that they are capable of capturing antinuclear antibodies in autoimmune disease patient serum.

First, the beads conjugated with the highest concentration of nuclear protein had the strongest fluorescence signal. In the overlay image of the beads, beads that captured ANA show high fluorescence but there were also some beads that captured low concentration of antinuclear antibodies.

As the concentration of nuclear protein decreased, the number of beads that captured ANA were reduced. For example, the beads conjugated with 0.3 mg/ml nuclear protein had the weakest fluorescence signal as shown in Figure 20.

As a negative control, beads conjugated with 3 mg/ml nuclear protein was incubated with ANA negative serum and very low fluorescence signal was observed as shown in Figure 21. This indicates that the developed beads are only specific to capture antinuclear antibodies. However, there was some non-specific binding between the nuclear protein and ANA negative antibodies. Few spots on the surface of microbeads showed fluorescence signal. This can be due to secondary antibody binding to the microbeads due to molecular interactions or due to antigens in nuclear protein recognized by the antibodies in the negative serum.

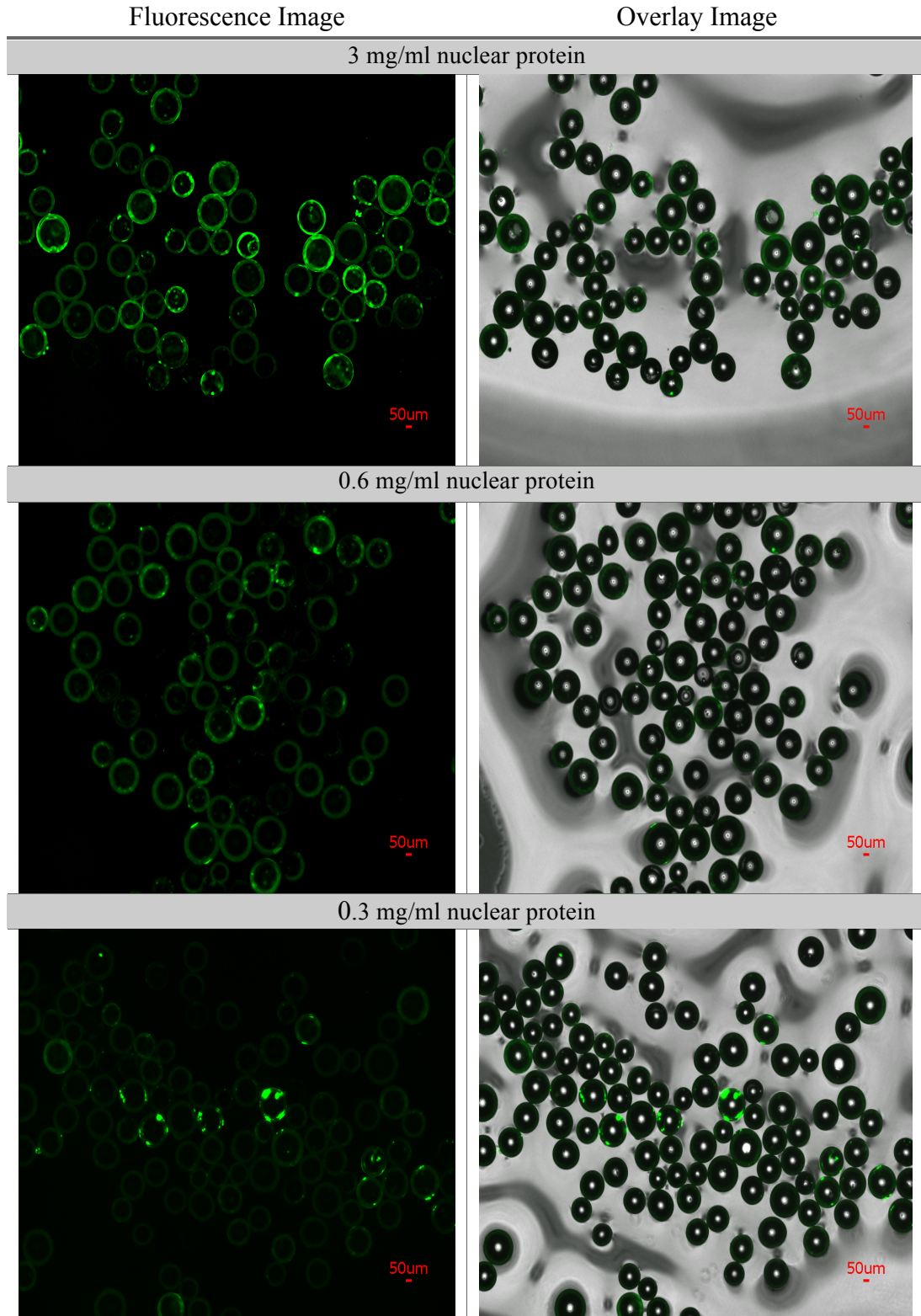


Figure 20 Effect of Decreasing nuclear protein concentration on the microbead's capturing capacity of ANA. As the concentration of nuclear protein conjugated to microbeads decreased, less number of microbeads captured ANA. The strongest fluorescence signal is observed from the beads conjugated with the highest concentration of nuclear proteins.

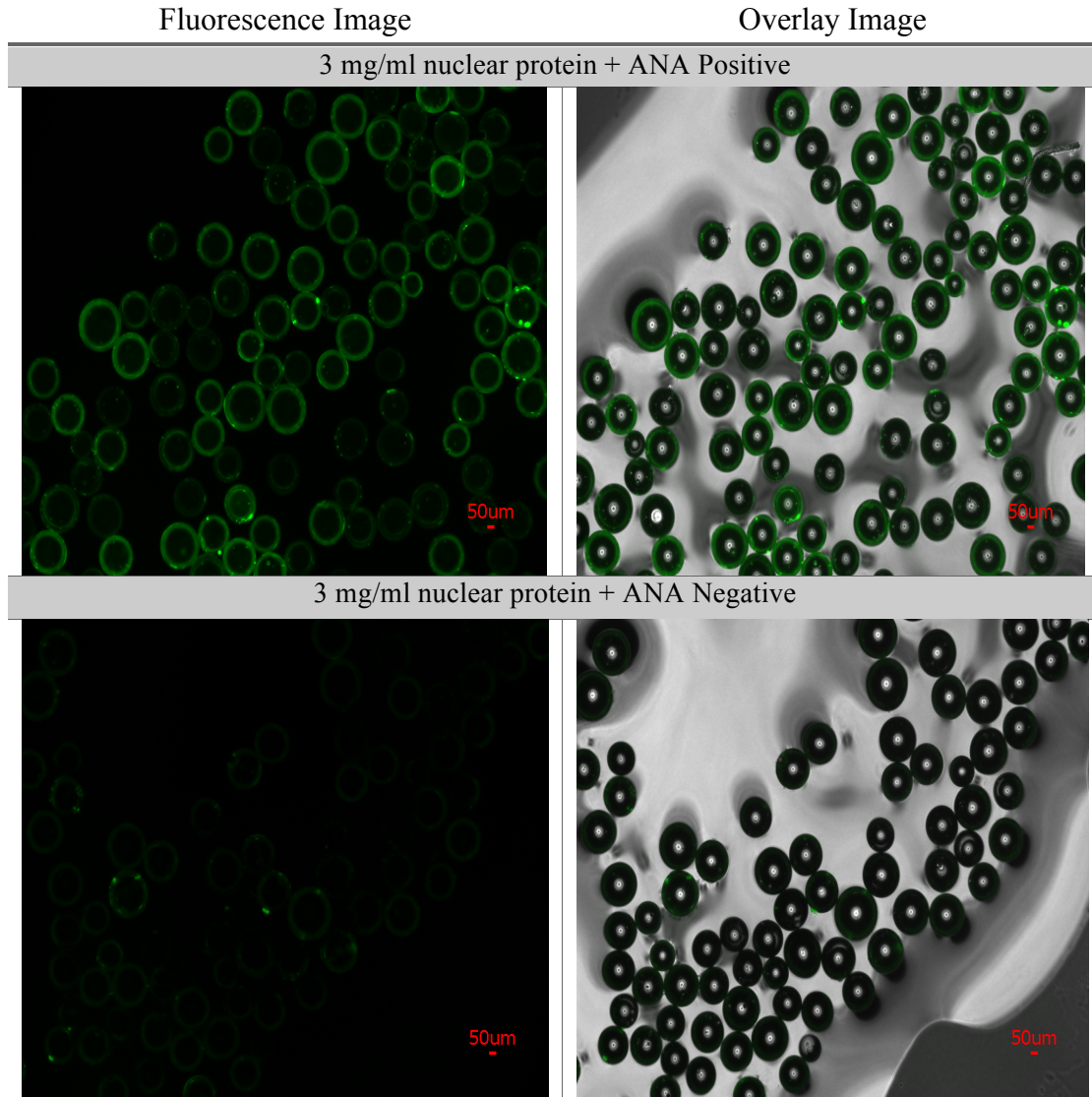
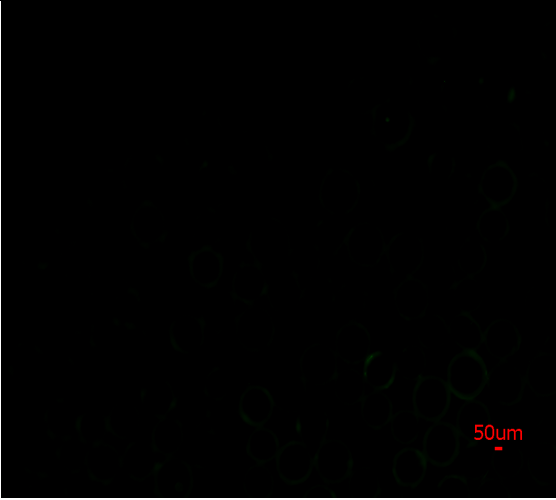
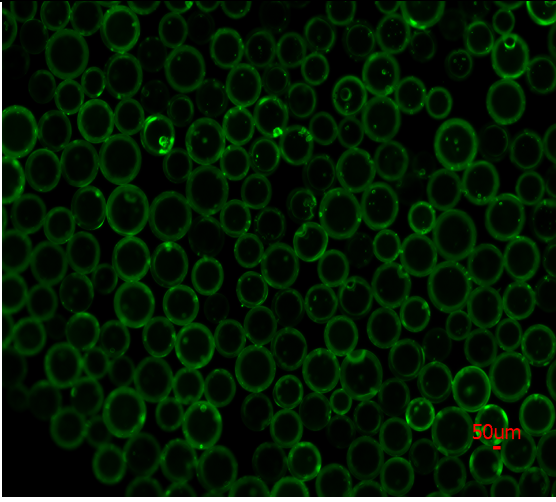
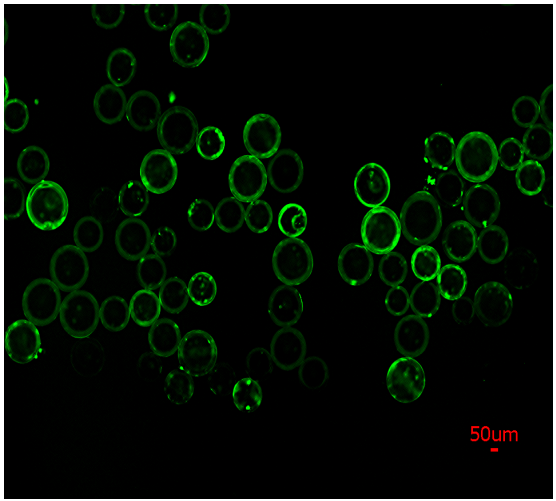


Figure 21 Comparison between microbeads that are conjugated with equal amount of nuclear protein in capturing ANA positive and negative antibodies. A strong fluorescence signal was observed from the beads incubated with ANA positive while no fluorescence was detected from the beads incubated with ANA negative human serum.

3.6. Fluorescence Image Analysis

3.6.1. Fluorescence Intensity of each image

In Figure 22, the fluorescence intensity and standard deviation of all images are represented.

No nuclear protein +BSA +anti-B-actin +FITC-labeled secondary antibody	Intensity	
	0.189	
	Standard Deviation	
0.6 mg/ml nuclear protein +BSA +anti-B-actin +FITC-labeled secondary antibody	Intensity	
	26.6	
	Standard Deviation	
3.0 mg/ml nuclear protein +BSA +ANA positive +FITC-labeled secondary antibody	Intensity	
	14.5	
	Standard Deviation	
	7.13	

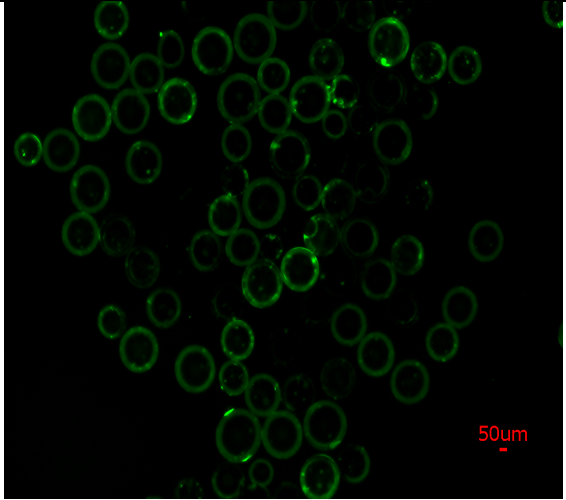
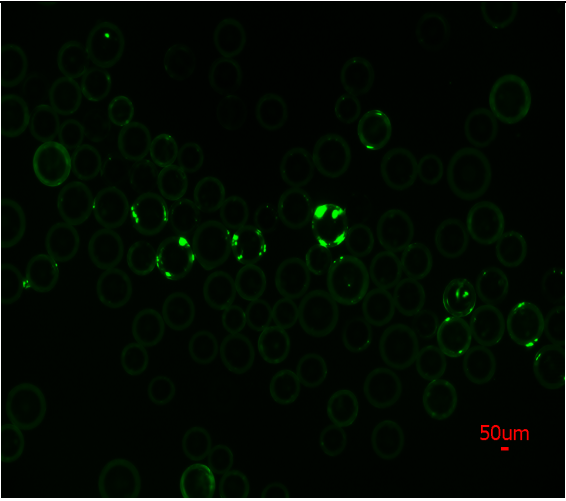
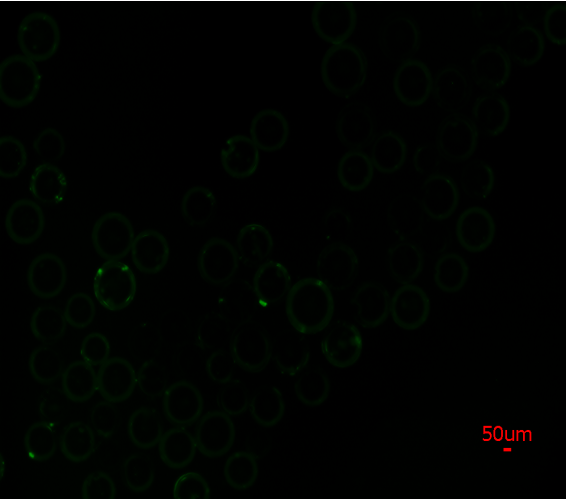
0.6 mg/ml nuclear protein +BSA +ANA positive +FITC-labeled secondary antibody	Intensity	
	10.1	
	Standard Deviation	
0.3 mg/ml nuclear protein +BSA +ANA positive +FITC-labeled secondary antibody	Intensity	
	5.23	
	Standard Deviation	
3.0 mg/ml nuclear protein +BSA +ANA negative +FITC-labeled secondary antibody	Intensity	
	1.21	
	Standard Deviation	
	3.01	

Figure 22 Fluorescence intensity and standard deviation of all images. As the nuclear protein concentration increased, the intensity increased. There was low fluorescence signal detected from the beads incubated with ANA negative serum.

As the concentration of nuclear protein increased, the intensity of fluorescence signal also increased. This represents that with higher concentration of nuclear proteins coupled to the beads, more ANAs were captured out. The standard deviation also increased because there was non-uniform coupling that some of the beads were not coupled with proteins. The fluorescence intensity of the beads incubated with ANA negative human serum was 1.21. This indicates that there was non-specific binding between the antibodies present in the serum and antigens from HEp-2 cell nuclear proteins. The beads coupled with no protein had intensity of 0.189 due to the background fluorescence from the FITC-labeled secondary antibodies. This intensity also correlates with result above that no proteins can bind to the beads after blocking with 5% BSA solution. However, some of the beads had non-uniform staining patterns that only portion of surface area had secondary antibody attached to it. This could be due to coupling issues that during incubation some beads stay at the bottom of the centrifuge tube and have no contact with the proteins.

3.6.2. Percent of beads showing fluorescence

In Table 2, the total number of beads and the number of beads that showed fluorescence above the threshold are presented. The number of beads that showed fluorescence decreased as the concentration of nuclear protein decreased. This correlates with the intensity analysis that when there are less proteins coupled to the beads, less amount of ANAs are captured out.

Table 2 Percentage of microbeads with fluorescence signal

	Total number of beads	Number of beads with fluorescence signal	% of beads showing fluorescence
No nuclear protein +BSA +anti-B-actin +FITC-labeled secondary antibody	0	0	0
0.6 mg/ml nuclear protein +BSA +anti-B-actin +FITC-labeled secondary antibody	214	202	94.3
3.0 mg/ml nuclear protein +BSA +ANA positive +FITC-labeled secondary antibody	73	64	87.7
0.6 mg/ml nuclear protein +BSA +ANA positive +FITC-labeled secondary antibody	87	72	82.7
0.3 mg/ml nuclear protein +BSA +ANA positive +FITC-labeled secondary antibody	89	18	20.2
3.0 mg/ml nuclear protein +BSA +ANA negative +FITC-labeled secondary antibody	76	3	3.94

3.7. Efficiency of Microbeads in Capturing Antinuclear Antibody

3.7.1. Calculation of microbead surface area

Using Equation (4) and (5), the number and surface area of microbeads depending on its mass is calculated as shown in Table 3.

Table 3 Number of beads and corresponding surface area based on the mass of microbeads

Mass of Microbeads (mg)	Number of Beads	Surface Area (cm ²)
4.5	524	1.03
9	1048	2.06
15	1747	3.43

3.7.2. ANA Concentration Difference Before and After incubation with the microbeads

The concentration of positive and negative ANA before and after incubation with microbeads are calculated as shown in Table 4.

Table 4 Change in concentration of ANA before and after incubation with the microbeads

Mass of Microbeads (mg)	Change in concentration of ANA before and after incubation with microbeads	
	ANA Positive	ANA Negative
4.5	34.7	5.4
9	59.9	16.8
15	84.8	29.1

As the number of beads conjugated with the same amount of nuclear proteins increased, the more ANAs were captured by the beads. In all groups, the microbeads were able to capture higher concentration of positive ANAs than

negative ANAs. A 15 mg of microbeads had the highest capturing capability. Some of negative ANAs were bound to the beads due to non-specific binding that antibodies in negative ANA serum recognized some of antigens in HEp-2 cell nuclear proteins.

3.7.3. Concentration of ANA per cm² of microbeads surface

The concentration of ANA captured by each cm² of microbead surface was calculated as shown in Table 5. The captured concentration of ANA was divided by the surface of microbeads in each group.

Table 5 Concentration of ANA per cm² of microbeads surface area

Mass of Microbeads (mg)	ANA Positive (µg/cm²)	ANA Negative (µg/cm²)
4.5	33.7	5.32
9	29.1	8.21
15	24.7	8.47
Average	29.2	7.33
Standard Deviation	4.49	1.74

In average, 29.2 µg of positive ANA was captured onto 1 cm² of microbead surface. On the other hand, an average of 7.33 µg negative ANA was captured onto 1 cm² of microbead surface. The difference between microbeads in capturing positive and negative ANAs were statistically significant with a p-value of 0.0318. This indicates that microbeads conjugated with nuclear proteins can significantly filter out positive ANAs compared to negative ANAs.

3.7.4. Comparison of ANA capturing efficiency between ELISA and Microbeads

Before comparison, the amount of ANAs captured by nuclear protein per 1 cm² of ELISA microtiter plate was calculated. Each well of 96 well-Maxisorp Immuno plate has a working surface area of 2.7 cm² (Thermo Fisher). The captured amount of ANA in each well was divided by the surface area as shown in Table 6 and 7.

Table 6 Concentration of captured ANA positive per cm² of microbeads surface area

Nuclear Protein Concentration (µg/ml)	Captured ANA Positive (µg)	Amount/cm² (µg/cm²)
0	0.00	0.00
20	4.48	1.66
40	5.46	2.02
80	7.72	2.86
160	10.64	3.94
Average	7.07	2.62
Standard Deviation	3.95	1.46

Table 7 Concentration of captured ANA negative per cm² of microbeads surface area

Nuclear Protein Concentration (µg/ml)	Captured ANA Negative (µg)	Amount/cm² (µg/cm²)
0	0.00	0.00
20	0.12	0.04
40	0.10	0.04
80	0.16	0.06
160	0.16	0.06
Average	0.13	0.05
Standard Deviation	0.07	0.0245

This result shows that in average 2.62 μg of positive ANA and 0.05 μg of negative ANA can be detected in 1 cm^2 of ELISA assay.

Table 8 Comparison between the microbeads and ELISA assay in capturing ANAs

	Amount/cm² ($\mu\text{g}/\text{cm}^2$)
ELISA: ANA Positive	2.62
ELISA: ANA Negative	0.05
Microbead: ANA Positive	29.2
Microbead: ANA Negative	7.33

In comparison to microbeads, ELISA assay has much lower binding capacity as shown in Table 8. For example, microbeads captured 24 μg more positive ANA than ELISA assay.

Using the microbeads, approximately 150 mg of microbeads have to be utilized to filter out 1 mg of ANAs in the patient serum. The amount includes 17470 microbeads and the surface area of 34 cm^2 .

CHAPTER 4

DISCUSSION

4.1. Extracted Nuclear Protein from HEp-2 Cells

The presence of nuclear protein was confirmed by the BCA and ELISA assay independently. The BCA assay quantified the concentration of nuclear proteins to be 3 mg/ml in 1 ml of PBS. This indicates that a total of 3 mg nuclear protein can be yielded from T175 flask culture.

The presence of nuclear protein was further analyzed by Indirect ELISA assay as shown in Figure 17. In this assay, different concentrations of nuclear proteins were coated to optimize the concentration of secondary antibodies and to generate a standard curve. As a primary antibody, anti- β -actin antibody was used because previous studies have found a high fraction of β -actin antigens in nuclear protein of HEp-2 cell lysate (Basu et al., 2015, Martinez et.al, 2009). The amount of anti- β -actin detected increased as the concentration of nuclear protein coated in each well increased. This shows that anti- β -actin and the extracted nuclear proteins are correlated, being specific to each other. Furthermore, anti- β -actin was not detected in the wells containing 0 μ g of nuclear protein. This shows that the non-specific binding was prevented by 5% BSA blocking solution. Thus, it can be stated that the extraction process was successful enough to yield pure nuclear fraction of proteins from HEp-2 cell lysate.

4.2. Determination of Specificity Between Nuclear Protein and Antinuclear Antibody

From the ELISA assay, the specificity between nuclear protein and ANA was confirmed. This was an important experimental step because ELISA assay validates the general idea of this study. If there is no specificity between the nuclear protein and ANA, the microbeads cannot capture any ANAs in human serum.

As shown in Figure 17 when the concentration of nuclear protein increases, the positive ANA captured in each well also increased. The same pattern was observed between anti- β -actin antibodies and nuclear proteins. The amount of anti- β -actin antibodies captured by nuclear proteins were higher in every concentration conditions. This is because β -actin are known to be very abundant in HEP-2 cell lysates, and there are less autoantigens that can be targeted by ANAs in the nuclear protein. Anti- β -actin antibodies were loaded as a positive control to ensure that ELISA assay was performed correctly.

However, a non-specific binding was still observed in the wells containing ANA negative serum as shown in Figure 16. This is because the nuclear protein from HEP-2 cells have few antigens that can be recognized by the negative serum. It is important to note that the concentration of ANA negative in each well did not increase when the nuclear protein concentration increased. This shows that the nuclear protein's specificity to ANA negative serum is not correlated.

From this result, the result of microbeads analysis could also be predicted. As no specificity between ANA negative and nuclear protein was observed in

ELISA assay, the nuclear proteins on the microbeads surface should not be capture negative ANAs as well.

4.3. Nuclear Protein Conjugation to the Microbeads

During the EDC/NHS reaction, if the carboxyl group on the microbeads becomes a stable amine-reactive ester, primary amine on protein from HEp-2 cell lysate can form a stable amide bond with the amine-reactive ester.

The fluorescence signal in Figure 19 represents that the nuclear protein was successfully conjugated to the bead. Because the negative control showed no fluorescence signal in Figure 18, it can be stated that blocking with 5% BSA solution effectively prevented non-specific binding. During the conjugation of nuclear protein to the microbeads, it is possible that some of binding sites remain open. By blocking these sites with BSA, the primary antibodies, in this case anti- β -actin antibodies can, only bind to the nuclear proteins on the bead's surface. In other studies, that use polystyrene carboxyl microbeads in similar size, blocking with 5% BSA solution was used to prevent non-specific binding (Sato).

4.4. Detection of Antinuclear Antibody using Microbeads

Microbeads conjugated with different concentrations of nuclear proteins all showed fluorescence signal. The fluorescence signal was stronger in beads conjugated with higher concentrations of nuclear proteins as shown in Figure 20.

This represents that microbeads conjugated with nuclear proteins were able to detect and capture ANAs in ANA positive human serum. The reason why fluorescence signal was higher in the beads conjugated with higher nuclear protein was because there were more ANAs bound to the beads, thus more secondary FITC-labeled antibodies were bound. HEP-2 cell substrates are known to contain more than 50 different types of antigens that are specific to ANAs (Giles et al., 2012). It is still unclear in which types reacted with nuclear proteins but higher nuclear protein concentration contained more binding sites for ANAs to bind.

The negative control, where beads were conjugated with 3 mg of nuclear proteins and were utilized to detect antibodies in ANA negative human serum, showed no fluorescence for two reasons. It is possible that no nuclear proteins were specific to ANA negative or the bound concentration of ANA negative was too low to detect fluorescence signal. This result correlated with the results from the ELISA assay where no specificity of nuclear proteins to negative ANAs was detected. Thus, it can be stated that the microbeads were specifically filtering out ANAs in ANA positive human serum.

4.5. Qualitative Analysis of the Microbead's Binding Capacity

The result showed that the microbeads could capture more ANAs than the ELISA. Microbeads conjugated with nuclear proteins detected an average of 29.2 μg ANAs per 1 cm^2 , while in ELISA an average of 2.62 μg ANAs were detected per 1 cm^2 of surface area. In both conditions, a low binding was observed in ANA

negative human serum because there were few antigens in HEP-2 cell substrate detected by negative ANAs.

The reason why microbeads can detect more ANAs than ELISA are because of larger surface area and flexible mobility of the antibodies. First, in the microbeads system, the surface area is greater than that of ELISA, which allows more contact between ANAs and nuclear proteins. Also, the volume of ANA positive human serum incubated with nuclear proteins are much higher in the microbeads system. For example, ELISA conducted in 96-well-plate can hold a volume up to 200 μ l whereas microbeads have no limitation in the incubation volume. In this study, 100 μ l of ANA positive human serum was added to each well in ELISA assay and 400 μ l of ANA positive human serum was added to each bead suspension for microbeads system. Since there are more ANAs available in the solution, the binding efficiency is greater in the microbeads.

Second, the microbeads provide a greater mobility of the antibodies and nuclear proteins. In ELISA assay, nuclear proteins are immobilized on the microtiter plate. The contactable area is very limited for ANAs to bind to the proteins. On the other hand, microbeads can move freely and assemble themselves in any direction. This allows more ANAs to bind to the bead and detected by the secondary antibodies.

To filter out 1 mg of ANAs in patient serum, approximately 150 mg of microbeads should be utilized based on the analysis. The average concentration of ANAs detected in patients positive to ANA is approximately 0.075 mg/ml (Hollingsworth et al., 1996). A normal adult has a blood volume of 5L. The total

quantity of ANAs in the patient positive to autoimmune disease is 375 mg. This means that to filter out 375 mg of ANAs, 56 g of microbeads must be added to the dialysis device. Due to the limited volume of a dialyzer, 56 g of microbeads could be too compact inside the filter. Thus, the coupling efficiency have to be improved to reduce the number of beads required for filtration.

CHAPTER 5

CONCLUSION

In this thesis, polystyrene carboxyl-linked microbeads (250 μm diameter) were utilized to detect and capture ANA in autoimmune disease patient serum. These beads were specially conjugated with nuclear proteins extracted from HEp-2 cells which are widely used as an autoimmune disease marker in the market. The results presented in this thesis clearly show that the microbeads can effectively filter out ANAs in autoimmune disease patient serum.

The current treatment involves immunosuppressive therapy which causes various side effects and economic burden for patients. Autoimmune disease patients regularly receive hemodialysis to balance out autoantibody level and remove excess fluid and waste. By applying the microbeads in the dialysis device, the elevated level of antinuclear antibodies in their blood can be easily decreased. By applying 150 mg of microbeads into the filtration device, at least 1 mg of ANAs can be filtered out. This is a simple, cost-effective and easily accessible therapy for all autoimmune disease patients.

In addition, the use of native autoantigen ensures that the reaction between the nuclear proteins and ANAs in the patients are accurate. In the currently marketed bead-based assays, synthetic or recombinant proteins are used. The recombinant autoantigens can include epitopes that are not present on native antigens. This can lead to undesired reactivity with the antibodies, interfering the filtration process.

CHAPTER 6

FUTURE WORK

6.1. Application of Microbeads in a Blood Filtration Device

The binding capacity of microbeads must be further analyzed in an actual blood filtration device. The number of beads, concentration of nuclear protein, and the stability of microbeads need to be determined because bench-scale reaction and the real-scale reaction can be very different. The flow rate of blood filtration and temperature can all affect antibody coupling to the microbeads. If the flow rate is too high, it is possible that the bond formed between ANA and nuclear proteins can be easily disrupted. Also, the blood filtration device has inlets and outlets where blood enters and leaves the device. The microbeads must not overflow into these inlets because the flow will be either blocked or slowed down.

6.2. Analysis of ANA Types Captured by Microbeads

In this thesis, the capability of microbeads in capturing ANA was mainly investigated. The analysis of captured ANA must be further analyzed to determine which types of ANAs are most specific and whether there is a capturing pattern in different autoimmune diseases. Also, a method to detach captured ANAs from the beads must be optimized. Currently, various buffers such as 20 mM MEMS or 1M Glycine solutions are usually used to decouple the bound antibodies. By trying

different buffers, detaching protocol should be optimized without destructing the antibody structure.

6.3. Application with Different Nuclear Proteins

In this thesis, only nuclear fraction from HEp-2 cells were used to detect ANAs. In many studies, other substrates such as *Crithidia luciliae* are also widely used to detect ANAs (Gerlach et al., 2015). Also, specific types of purified autoantigens can be coupled to the microbeads for customized therapy. Some autoimmune disease patients have high level of one or two specific autoantibodies. The microbeads coupled with corresponding autoantigens may be used to filter out these antibodies in the patient serum.

6.4. Change of Coupling Buffer and Incubation Apparatus

In few studies, EDC/NHS reaction was performed in MEMS buffer instead of PBS. This is because an intermediate formed by EDC/NHS can be much stable in MEMS buffer (Bale et al., 2014). For next trial, the buffer should be changed to see whether binding efficiency can be improved. In this study, the microbeads were incubated in 1.7 mL of micro centrifuge tube. The effect of incubation volume should also be analyzed. If the volume of tube is increased, the binding efficiency will probably increase because the proteins and antibodies have more flexible mobility.

Reference

1. Aleksandrova, E., Verijnikova, Z., Novikov, A., Panafidina, T., Seredavkina, N., Popkova, T., ... & Nasonov, E. (2016). THU0257 Diagnostic Accuracy of Multiplex Bead-Based Immunoassay for Antinuclear Antibodies (ANA) Testing in Systemic Lupus Erythematosus (SLE). *Annals of the Rheumatic Diseases*, 75(Suppl 2), 281-281.
2. Bale, S. S., Price, G., Casali, M., Saeidi, N., Bhushan, A., & Yarmush, M. L. (2014). A highly sensitive microsphere-based assay for early detection of Type I diabetes. *Technology*, 2(03), 200-205.
3. Baronaite, R., Engelhart, M., Mørk Hansen, T., Thamsborg, G., Slott Jensen, H., Stender, S., & Szecsi, P. B. (2014). A comparison of anti-nuclear antibody quantification using automated enzyme immunoassays and immunofluorescence assays. *Autoimmune diseases*, 2014.
4. Basu, A., Woods-Burnham, L., Ortiz, G., Rios-Colon, L., Figueroa, J., Albesa, R., ... & Casiano, C. A. (2015). Specificity of antinuclear autoantibodies recognizing the dense fine speckled nuclear pattern: Preferential targeting of DFS70/LEDGFp75 over its interacting partner MeCP2. *Clinical Immunology*, 161(2), 241-250.
5. Buchner, C., Bryant, C., Eslami, A., & Lakos, G. (2014). Anti-nuclear antibody screening using HEP-2 cells. *JoVE (Journal of Visualized Experiments)*, (88), e51211-e51211.
6. Ceribelli, A., Satoh, M., & Chan, E. K. (2013). Antinuclear Antibodies. In *Autoantibodies: Third Edition*. Elsevier BV.

7. Chan, E. K., Burlingame, R. W., & Fritzler, M. J. (2016). Detection of Autoantibodies by Enzyme-Linked Immunosorbent Assay and Bead Assays. In *Manual of Molecular and Clinical Laboratory Immunology, Eighth Edition* (pp. 859-867). American Society of Microbiology.
8. Chandrashekhara, S. (2012). The treatment strategies of autoimmune disease may need a different approach from conventional protocol: A review. *Indian journal of pharmacology*, 44(6), 665.
9. Copple, S. S., Martins, T. B., Masterson, C., Joly, E., & Hill, H. R. (2007). Comparison of three multiplex immunoassays for detection of antibodies to extractable nuclear antibodies using clinically defined sera. *Annals of the New York Academy of Sciences*, 1109(1), 464-472.
10. Cucchiari, D., Graziani, G., & Ponticelli, C. (2014). The dialysis scenario in patients with systemic lupus erythematosus. *Nephrology Dialysis Transplantation*, 29(8), 1507-1513.
11. Dasgupta, M. K. (2000). Exit-site and catheter-related infections in peritoneal dialysis: Problems and progress. *Nephrology*, 5(1-2), 17-25.
12. Darrah, E., Rosen, A., Giles, J.T. and Andrade, F., 2012. Peptidylarginine deiminase 2, 3 and 4 have distinct specificities against cellular substrates: novel insights into autoantigen selection in rheumatoid arthritis. *Annals of the rheumatic diseases*, 71(1), pp.92-98.
13. Dey, I. D., & Isenberg, D. A. Autoimmune Disease: Diagnosis. *eLS*.

14. D. Pisetsky, G. Gilkeson, E. William St Clair, (1997), SYSTEMIC LUPUS ERYTHEMATOSUS : Diagnosis and Treatment. Medical Clinics of North America 81(1), 113–128
15. Fhied, C., Kanangat, S., & Borgia, J. A. (2014). Development of a bead-based immunoassay to routinely measure vimentin autoantibodies in the clinical setting. *Journal of immunological methods*, *407*, 9-14.
16. Giles, S. R., Copple, S. S., Giles, S. R., Jaskowski, T. D., Gardiner, A. E., Wilson, A. M., & Hill, H. R. (2012). Screening for IgG antinuclear autoantibodies by HEp-2 indirect fluorescent antibody assays and the need for standardization. *American journal of clinical pathology*, *137*(5), 825-830.
17. Gerlach, S., Affeldt, K., Pototzki, L., Krause, C., Voigt, J., Fraune, J., & Fechner, K. (2015). Automated evaluation of Crithidia luciliae based indirect immunofluorescence tests: a novel application of the EUROPattern-Suite technology. *Journal of immunology research*, 2015.
18. Goldberg, R. J. (1952). A Theory of Antibody—Antigen Reactions. I. Theory for Reactions of Multivalent Antigen with Bivalent and Univalent Antibody². *Journal of the American Chemical Society*, *74*(22), 5715-5725.
19. Hauser, A. B., Stingham, A. E., Kato, S., Bucharles, S., Aita, C., Yuzawa, Y., & Pecoits-Filho, R. (2008). Characteristics and causes of immune dysfunction related to uremia and dialysis. *Peritoneal Dialysis International*, *28*(Supplement 3), S183-S187.
20. Hayashi, N., Kawamoto, T., Mukai, M., Morinobu, A., Koshiba, M., Kondo, S., ... & Kumagai, S. (2001). Detection of antinuclear antibodies by use of an

- enzyme immunoassay with nuclear HEp-2 cell extract and recombinant antigens: comparison with immunofluorescence assay in 307 patients. *Clinical Chemistry*, 47(9), 1649-1659.
21. Hiemann, R., Büttner, T., Krieger, T., Roggenbuck, D., Sack, U., & Conrad, K. (2009). Challenges of automated screening and differentiation of non-organ specific autoantibodies on HEp-2 cells. *Autoimmunity Reviews*, 9(1), 17-22.
22. Heneghan, M. A., & McFarlane, I. G. (2002). Current and novel immunosuppressive therapy for autoimmune hepatitis. *Hepatology*, 35(1), 7-13.
23. Himoto, T., & Nishioka, M. (2013). Autoantibodies in liver disease: important clues for the diagnosis, disease activity and prognosis. *Autoimmunity Highlights*, 4(2), 39-53.
24. Hollingsworth, P. N., Dawkins, R. I., & Peter, J. B. (1996). Precise quantitation of antinuclear antibodies on HEp-2 cells without the need for serial dilution. *Clinical and diagnostic laboratory immunology*, 3(4), 374-377.
25. Jaskowski, T. D., Gardiner, A. E., Wilson, A. M., & Hill, H. R. (2012). Screening for IgG antinuclear autoantibodies by HEp-2 indirect fluorescent antibody assays and the need for standardization. *American journal of clinical pathology*, 137(5), 825-830.
26. Kavanaugh, A., Tomar, R., Reveille, J., Solomon, D. H., & Homburger, H. A. (2000). Guidelines for clinical use of the antinuclear antibody test and tests for specific autoantibodies to nuclear antigens. *Archives of pathology & laboratory medicine*, 124(1), 71-81.

27. Keren, DF (June 2002). "Antinuclear antibody testing". *Clinics in laboratory medicine*. **22** (2): 447–74.
28. Kronbichler, A., & Mayer, G. (2013). Renal involvement in autoimmune connective tissue diseases. *BMC medicine*, *11*(1), 95.
29. Kuwana, M., Kimura, K., Hirakata, M., Kawakami, Y., & Ikeda, Y. (2002). Differences in autoantibody response to Th/To between systemic sclerosis and other autoimmune diseases. *Annals of the rheumatic diseases*, *61*(9), 842-846.
30. Kumar, Y., Bhatia, A., & Minz, R. W. (2009). Antinuclear antibodies and their detection methods in diagnosis of connective tissue diseases: a journey revisited. *Diagnostic pathology*, *4*(1), 1.
31. Lange, S., Gögel, S., Leung, K.Y., Vernay, B., Nicholas, A.P., Causey, C.P., Thompson, P.R., Greene, N.D. and Ferretti, P., 2011. Protein deiminases: new players in the developmentally regulated loss of neural regenerative ability. *Developmental biology*, *355*(2), pp.205-214.
32. Lauren Martz, 2015. Padlocks Keys to Academia. Biocentury Innovations. Retrieved from <http://www.padlocktherapeutics.com/wp-content/uploads/2015/05/BioCentury-Innovations-Padlock-30April15.pdf>
33. Mahler, M., Meroni, P. L., Bossuyt, X., & Fritzler, M. J. (2014). Current concepts and future directions for the assessment of autoantibodies to cellular antigens referred to as anti-nuclear antibodies. *Journal of immunology research*, 2014.
34. Marrack, P., Kappler, J., & Kotzin, B. L. (2001). Autoimmune disease: why and where it occurs. *Nature medicine*, *7*(8), 899.

35. Martins, T. B., Burlingame, R., von Mühlen, C. A., Jaskowski, T. D., Litwin, C. M., & Hill, H. R. (2004). Evaluation of multiplexed fluorescent microsphere immunoassay for detection of autoantibodies to nuclear antigens. *Clinical and diagnostic laboratory immunology*, *11*(6), 1054-1059.
36. Martínez, I., Lombardía, L., Herranz, C., García-Barreno, B., Domínguez, O., & Melero, J. A. (2009). Cultures of HEp-2 cells persistently infected by human respiratory syncytial virus differ in chemokine expression and resistance to apoptosis as compared to lytic infections of the same cell type. *Virology*, *388*(1), 31-41.
37. Moscarello, M. A., Mastronardi, F. G., & Wood, D. D. (2007). The role of citrullinated proteins suggests a novel mechanism in the pathogenesis of multiple sclerosis. *Neurochemical research*, *32*(2), 251-256.
38. Meroni, P. L., & Schur, P. H. (2010). ANA screening: an old test with new recommendations. *Annals of the rheumatic diseases*, annrheumdis127100.
39. Osborn, T. G., Patel, N. J., Moore, T. L., & Zuckner, J. (1984). Use of the HEp-2 cell substrate in the detection of antinuclear antibodies in juvenile rheumatoid arthritis. *Arthritis & Rheumatism*, *27*(11), 1286-1289.
40. Peene, I., Meheus, L., Veys, E. M., & De Keyser, F. (2001). Detection and identification of antinuclear antibodies (ANA) in a large and consecutive cohort of serum samples referred for ANA testing. *Annals of the rheumatic diseases*, *60*(12), 1131-1136.
41. Premawardhana, L. D. K. E., & Lazarus, J. H. (2006). Management of thyroid disorders. *Postgraduate medical journal*, *82*(971), 552-558.

42. Rigon, A., Soda, P., Zennaro, D., Iannello, G., & Afeltra, A. (2007). Indirect immunofluorescence in autoimmune diseases: assessment of digital images for diagnostic purpose. *Cytometry Part B: Clinical Cytometry*, 72(6), 472-477.
43. Ronco, C., Ghezzi, P. M., Brendolan, A., Crepaldi, C., & La Greca, G. (1998). The haemodialysis system: basic mechanisms of water and solute transport in extracorporeal renal replacement therapies. *Nephrology Dialysis Transplantation*, 13(6), 3-9.
44. Sack, U; Conrad, K; Csernok, E; Frank, I; Hiepe, F; Krieger, T; Kromminga, A; Landenberg, Pv; Messer, G; Witte, T; Mierau, R (June 2009). die deutsche EASI-Gruppe (European Autoimmunity Standardization, Initiative). "Autoantibody detection by indirect immunofluorescence on HEp-2 cells
45. Sato, K., Tokeshi, M., Odake, T., Kimura, H., Ooi, T., Nakao, M., & Kitamori, T. (2000). Integration of an immunosorbent assay system: analysis of secretory human immunoglobulin A on polystyrene beads in a microchip. *Analytical chemistry*, 72(6), 1144-1147.
46. Satoh, M., Vázquez-Del Mercado, M., & Chan, E. K. (2009). Clinical interpretation of antinuclear antibody tests in systemic rheumatic diseases. *Modern rheumatology*, 19(3), 219-228.
47. Schmidt, E., Seitz, C. S., Benoit, S., Bröcker, E. B., & Goebeler, M. (2007). Rituximab in autoimmune bullous diseases: mixed responses and adverse effects. *British Journal of Dermatology*, 156(2), 352-356.

48. Shovman, O., Gilburd, B., Zandman-Goddard, G., Yehiely, A., Langevitz, P., & Shoenfeld, Y. (2005). Multiplexed AtheNA multi-lyte immunoassay for ANA screening in autoimmune diseases. *Autoimmunity*, 38(1), 105-109.
49. Smith, J., Onley, D., Garey, C., Crowther, S., Cahir, N., Johanson, A., ... & Swarbrick, P. (2005). Determination of ANA specificity using the UltraPlex™ platform. *Annals of the New York Academy of Sciences*, 1050(1), 286-294.
50. Tan, E. M. (1989). Antinuclear antibodies: diagnostic markers for autoimmune diseases and probes for cell biology. *Advances in immunology*, 44, 93-151.
51. Teo C, Shave S, Chor A, Salleh A, Rahman M, Walkinshaw M and Tejo B, 2012. Discovery of a new class of inhibitors for the protein arginine deiminase type 4 (PAD4) by structure-based virtual screening. *BMC Bioinformatics*, 13(Suppl 17):S4
52. Yamasaki Y, Honkanen-Scott M, Hernandez L, Ikeda K, Barker T, Bubb MR, et al. Nucleolar staining cannot be used as a screening test for the scleroderma marker anti-RNA polymerase I/III antibodies. *Arthritis Rheum*. 2006;54:3051–6.
53. Xu, M., Roberts, B. B., Busby, B. A., Jack, R. M., Finn, L. S., Emery, H. M., & Rutledge, J. C. (2007). Evaluation of multiplex antinuclear antibody assay in pediatric patients. *Laboratory Medicine*, 38(11), 671-675.
54. MS statistics. Retrieved from <https://multiplesclerosis.net/what-is-ms/statistics/>.
55. Autoimmune statistics, AARDA. <http://www.aarda.org/autoimmune-information/autoimmune-statistics/>.

56. Antinuclear Antibodies Nuclear Staining Image., MBL International Inc.,
<https://www.mblintl.com/products/ank-120>.
57. EDC/NHS Reaction Mechanism, Thermo Fisher.,
<https://www.thermofisher.com/content/dam/LifeTech/Images/integration/01-Carbodiimide-Sulfo-NHS-Rxn.jpg>.
58. Indirect ELISA Protocol., Abcam.,
<http://www.abcam.com/ps/pdf/protocols/indirect%20elisa%20protocol.pdf>.
59. Characteristics of Polystyrene Particles., Spherotech., 2016.
60. Hemodialysis image., <http://drsatishd.com/hemodialysis-process/>.
61. Hemodialysis Diffusion image., GAMBRO, PrismaFlex Continuous Renal Replacement Therapy Principles, 2007, <https://image.slidesharecdn.com/1-prismaflexcrrtintro-seg12007-110326040426-phpapp02/95/1-prismaflex-crrt-intro-seg-1-2007-17-728.jpg?cb=1301112387>